

Subharmonic Sideband Separating Schottky Diode Mixer for Submillimetre Wave Applications

PETER SOBIS

Physical Electronics Laboratory

Department of Microtechnology and Nanoscience – MC2

CHALMERS UNIVERSITY OF TECHNOLOGY

Gothenburg, Sweden 2010

THESIS FOR THE DEGREE OF LICENTIATE OF ENGINEERING

Subharmonic Sideband Separating Schottky Diode Mixer for Submillimetre Wave Applications

Peter Sobis



Physical Electronics Laboratory
Department of Microtechnology and Nanoscience - MC2
Chalmers University of Technology
Göteborg, Sweden, April 2010

Subharmonic Sideband Separating Schottky Diode Mixer for Submillime- tre Wave Applications

PETER SOBIS

© Peter Sobis, 2010

Chalmers University of Technology
Department of Microtechnology and Nanoscience - MC2
Physical Electronics Laboratory
SE-412 96 Göteborg , Sweden
Telephone +46 (0)31-772 1000

ISSN 1652-0769
Technical report MC2-168

Printed by Chalmers Reproservice,
Göteborg, Sweden, 2010

Abstract

The submillimetre wave band withholds a wealth of molecular information in the form of spectral lines, originating from transitions between rotational and vibrational modes. By studying the shape of the spectral lines the physical conditions of the observed species, such as temperature, wind and pressure can be found. Radiometry is used in atmospheric research for extraction of the emission line frequency spectra. By the use of limb-sounding techniques, where the limb of the Earth's atmosphere is scanned, the vertical distribution of gases can be resolved. This enables the study of the chemical exchange mechanisms between the atmospheric layers, processes that have implications on our climate and environment.

In this thesis an integrated room temperature sideband separating receiver topology for future Earth atmospheric instruments is presented. The possibility to separate the receiver sidebands is important when spectral lines originating from the receiver upper and lower sidebands, interfere with each other in the downconverted IF band.

The proposed 2SB receiver topology is based on a subharmonic IQ-mixer consisting of two subharmonic ($\times 2$) Schottky diode DSB Mixers, two IF LNA MMIC's and LO and RF 90 degree waveguide hybrids. The IQ-mixer together with an IF 90 degree hybrid or an IQ-correlator spectrometer, makes the separation of the sidebands possible. The developed mixer has the advantage of low RF and LO VSWR as 90 degree hybrids are used, leading to improved performance compared to other topologies. With an experimental modular sideband separating mixer assembly, applying only a fixed phase tuning of the I and Q signals in 3 GHz IF bands, image rejection levels around 20 dB have been reached over the whole band.

Moreover two novel concepts for the realisation of differential phase shifters are presented. The phase shifters are based on very simple and compact filter structures with a minimum lateral distribution. Thereto the filter structures themselves can be used for signal distribution, leading to very efficient designs suitable for MMIC technology and submillimetre circuits.

A TRL-calibration methodology applicable for Terahertz Monolithic Integrated Circuits TMIC's, is also proposed. The design of a waveguide packaged membrane based TMIC TRL-kit is presented, which can be used for S-parameter characterisation of submillimetre devices and circuits.

Keywords: submillimetre wave technology, heterodyne receivers, Schottky diodes, subharmonic mixers, sideband separation, radiometers, phase shifters, differential phase shifters, S-parameter measurements, TRL-calibration

List of publications

Appended papers

- [A] P. Sobis, J. Stake and A. Emrich, “A 170 GHz 45° Hybrid for Submillimeter Wave Sideband Separating Subharmonic Mixers,” *IEEE Microwave and Wireless Components Letters*, vol. 18, no. 10, pp. 680–682, Oct. 2008.
- [B] P. Sobis, J. Stake and A. Emrich, “High/Low Impedance Transmission Line and Coupled Line Filter Networks for Differential Phase Shifters,” submitted to *IEEE Transactions on Microwave Theory and Techniques*, Feb. 2010.
- [C] H. Zhao, A.-Y. Tang, P. Sobis, T. Bryllert, K. Yhland, J. Stenarson and J. Stake “TRL-Calibration and S-Parameter Characterization of Membrane Circuits for Submillimeter Wave Frequencies,” submitted to *IEEE Microwave and Wireless Components Letters*, Mar. 2010.
- [D] P. Sobis, A. Olsen, J. Vukusic, V. Drakinskiy, S. Cherednichenko, A. Emrich and J. Stake, “Compact 340 GHz Receiver Front-Ends,” *20th International Symposium on Space Terahertz Technology, ISSTT 2009, Charlottesville, VA, USA*, pp. 183–189, Apr. 2009.
- [E] P. Sobis, A. Emrich and M. Hjorth, “STEAMR Receiver Chain,” *20th International Symposium on Space Terahertz Technology, ISSTT 2009, Charlottesville, VA, USA*, pp. 320–325, Apr. 2009.
- [F] A. Emrich, S. Andersson, M. Wannerbratt, P. Sobis, S. Cherednichenko, D. Runesson, T. Ekebrand, M. Krus, C. Tegnander and U. Krus, “Water Vapor Radiometer for ALMA,” *20th International Symposium on Space Terahertz Technology, ISSTT 2009, Charlottesville, VA, USA*, pp. 174–177, Apr. 2009.

Other publications

- [a] H. Zhao, A. Tang, P. Sobis, V. Drakinskiy, T. Bryllert and J. Stake, “Characterisation of GaAs Membrane Circuits for THz Heterodyne Receiver Applications,” *ISSTT, Oxford, UK, 2010*.
- [b] A. Tang, P. Sobis, V. Drakinskiy, H. Zhao and J. Stake, “Parameter Extraction and Geometry Optimisation of Planar Schottky Diodes,” *ISSTT, Oxford, UK, 2010*.
- [c] H. Zhao, A. Tang, P. Sobis, V. Drakinskiy, T. Bryllert and J. Stake, “340 GHz GaAs Monolithic Membrane Supported Schottky Diode Circuits,” *GigaHertz Symposium, Lund, Sweden, 2010*.
- [d] R. Dahlbäck, B. Banik, P. Sobis, A. Fhager, P. Persson and J. Stake, “A Compact 340 GHz Heterodyne Imaging System,” *GigaHertz Symposium, Lund, Sweden, 2010*.
- [e] P. Sobis, A. Emrich and M. Hjorth, “Receiver Chain for the STEAMR Instrument,” *4th ESA Workshop on Millimetre Wave Technology and Applications, ESTEC, the Netherlands, 2009*.
- [f] P. Sobis, T. Bryllert, A.Ø. Olsen, J. Vukusic, V. Drakinskiy, S. Cherednichenko, J. Stake and A. Emrich, “Development of a compact 340 GHz Receiver Front-End,” *4th ESA Workshop on Millimetre Wave Technology and Applications, ESTEC, the Netherlands, 2009*.
- [g] P. Sobis, J. Stake and A. Emrich, “Towards a THz Sideband Separating Subharmonic Schottky Mixer,” *ISSTT, Groningen, the Netherlands, 2008*.
- [h] P. Sobis, J. Stake and A. Emrich, “Towards a THz Sideband Separating Subharmonic Schottky Mixer,” *GigaHertz Symposium, Goteborg, Sweden, 2008*.
- [i] P. Sobis, J. Stake and A. Emrich, “Design of a Subharmonic 340 GHz GaAs Schottky Diode Mixer on Quartz with Integrated Planar LO-IF Duplexer,” *4th ESA Workshop on Millimetre Wave Technology and Applications, Espoo, Finland, 2006*.

- [j] P. Sobis, J. Stake and A. Emrich, "A simple comparison of VDI and UMS GaAs Schottky diodes for subharmonic mixers in the lower THz band," *30th Workshop on Compound Semiconductors Devices and Integrated Circuits, WOCSDICE, Fiskebäckskil, Sweden 2006.*
- [k] P. Sobis, J. Stake and A. Emrich, "Optimisation and Design of a Suspended Subharmonic 340 GHz Schottky Diode Mixer," *IRMMW-THz Symposium, Shanghai, China, 2006.*
- [l] P. Sobis, J. Stake and A. Emrich, "A 110 GHz GaAs Schottky Diode Mixer Design on Quartz with Planar LO Feed," *GigaHertz Symposium, Uppsala, Sweden, 2005.*

Notations and abbreviations

Notations

C	Capacitance
I	Current
k_B	Boltzmann's constant
L	Inductance
q	Electron charge
R	Electrical resistance
T	Temperature
V	Voltage
η	Diode ideality factor

Abbreviations

CAD	Computer Aided Design
CL	Conversion Loss
CMB	Cosmic Microwave Background
CPW	Co-Planar Waveguide
CW	Continuous Wave
DSB	Double Side Band
EM	Electro Magnetic
ESA	European Space Agency
FET	Field Effect Transistor
FOM	Figure-Of-Merit
HB	Harmonic Balance
HBV	Heterostructure Barrier Varactor
IC	Integrated Circuit

IF	Intermediate Frequency
IR	Infrared
LN	Liquid Nitrogen
LNA	Low Noise Amplifier
LO	Local Oscillator
MIC	Monolithic Integrated Circuit
MMIC	Microwave Monolithic Integrated Circuit
PLL	Phase-Locked Loop
RF	Radio Frequency
RT	Room Temperature
SD	Schottky Diode
SHIQ	SubHarmonic IQ
SHIRM	SubHarmonic Image Rejection Mixer
SHM	SubHarmonic Mixer
SSB	Single Side Band
Submm	Submillimetre
TMIC	Terahertz Monolithic Integrated Circuit
VCO	Voltage-Controlled Oscillator
VSWR	Voltage Standing Wave Ratio
WVR	Water Vapor Radiometer
2SB	Sideband Separating, Dual Sideband

Contents

Abstract	i
List of publications	iii
Notations and abbreviations	vii
1 Introduction	1
1.1 Background	1
1.2 Motivation and main results	3
2 Radiometer systems	7
3 Diode mixers	11
3.1 Mixer theory	11
3.2 Schottky diodes	13
3.3 Noise theory	15
4 Design of subharmonic mixer	17
4.1 Circuit technology considerations	17
4.2 Subharmonic (x2) mixer topologies	19
4.3 E-field coupled rectangular waveguide to planar trans- mission line transitions	19
4.4 Planar filter structures	21
4.5 3D-modeling of diode	22
4.6 Diode embedding impedances	23
4.7 LO/IF filter circuit	23
4.8 LO matching circuit	25
4.9 RF matching circuit	26
4.10 Mixer circuit modeling	26
4.11 2SB mixer design	28
5 Characterisation of mixers	31
5.1 Noise measurements	31
5.2 Image rejection measurements	34
5.3 CW conversion loss measurements	36

6 Conclusions and future outlook	39
Acknowledgements	41
Bibliography	43

Chapter 1

Introduction

For future THz applications, a versatile and flexible receiver technology is needed, enabling true system integration, reducing cost and size and adding to the system functionality. This can only be done at component level and includes novel circuit integration schemes, packaging concepts as well as finding new measurement and characterisation techniques.

This research project aims at developing new THz receiver topologies based on GaAs Schottky diode technology [1–4], enabling new types of instruments and applications. Attention is given to system integration and reliability aspects as well as cost, for the possibility to transfer results directly to industrial applications. The idea is to set new standards for subsystem functionality for THz frequencies and to make it possible to define instruments focused on end user needs and requirements, instead of what is possible to implement on a component level today. In particular the main goal has been to develop a 2SB receiver topology, employing subharmonic Schottky diode mixers, for the STEAMR instrument [5], with an operating frequency band of around 320 GHz to 360 GHz. Such a device comes to a high cost due to its complexity, however on system level, it will actually reduce the complexity considerably and enable new and more efficient instrument configurations.

1.1 Background

Radio astronomy has indisputably been the main driver in the development of sensitive detectors operating in the submillimetre wave range [6, 7], i.e. the electromagnetic spectrum from 300 GHz to 3 THz. Today we find advanced submillimetre wave radio telescopes like the ALMA interferometer project [8] and its precursor the APEX telescope [9], the Herschel Space Observatory [10] and COBE [11], dedicated for exploration of various aspects of the universe. The submillimetre wave band, constituting the lower part of the THz frequency band, is of great importance, as it contains a large portion of the emission and

absorption lines [12], originating from rotational and vibrational modes of basic molecules. An important part of the cosmic microwave background (CMB) radiation, originating from the very early years after Big Bang, is also found in this frequency range. Furthermore, the potential of THz-technology for new applications in the fields of medicine, security, etc., is being explored [13]. So far, one of the main obstacles has been the high development costs of THz systems. Therefore, the way towards consumer applications seems still long. A promising candidate for true commercialisation of THz technology is silicon technology [14].

At present, ultimate low noise receivers used for radio astronomy are based on cryogenic devices such as Superconductor-Insulator-Superconductor (SIS) tunnel junctions [15] and Hot Electron Bolometers (HEB's) [16] reaching quantum noise levels. The development of these innovative devices has been possible thanks to advancements in processing techniques for micro and nano-scale electronics, the increase in available computational power and through the development of sophisticated CAD software. Thereto, the advancement of THz source technology and development of compact broadband source modules, using solid state amplifiers [17] and diode multipliers [18], has greatly improved the usability of heterodyne radio receivers.

Another important application of radiometry is atmospheric sensing and earth observations [19]. Important parameters such as temperature, pressure, wind speed and gas concentration can be extracted by studying the shape of the spectral lines. Atmospheric sensing of the Earth is possible through ground based observations [20], air-born high altitude observations from aeroplanes [21, 22], balloons [23] and sounding rockets [24], and by the use of space-born limb sounders and imagers [25]. In contrast to radio astronomy observations, Earth observations are typically characterized by high brightness temperatures and short integration times [26]. Earth observations are also ideally made continuously (on a daily or weekly basis) during many years (>7), to accommodate for changes in between winter and summer as well as for naturally occurring irregularities in the climate cycle. It is then possible to detect trends and make future predictions of the climate development [5]. In the study of the chemical processes that control our climate, resolving the vertical distribution of key trace gases is important, as it gives insights to the chemical interaction between the different atmospheric layers and because the impact of molecules differ depending on the altitude they are at. The most efficient way of extracting detailed vertical information is by using limb sounding techniques, i.e. by scanning the Earth's limb, layer by layer. For continuous monitoring this is ideally done using space born instruments as large parts of the atmosphere can be covered by a single satellite.

Atmospheric sensing has proven to be possible through the use of less sensitive receivers such as those based on room temperature (RT) GaAs Schottky diode technology. Being the predecessor of modern cryogenic technology, GaAs Schottky diodes have a long track record and can be considered as low risk, high reliability alternative. The trade off in-between scientific impact and cost makes the use of room temperature technology very attractive, as the complexity of test equipment and facilities as well as test procedures is reduced, compared to cryogenic receiver development. Also the choice of materials, assembly procedures and more important the instrument design are simplified considerably. Schottky based receiver systems can be made very compact (low weight) and have no fundamental limitations in the operation lifetime, i.e. not limited by the amount of cooling agent that can be brought on board the satellite, which cryogenic devices typically are [11, 27], even though active closed cycle cryogenic cooling systems like for SPICA [28] are being developed, reducing the weight of the satellite dramatically.

1.2 Motivation and main results

At submillimetre wave frequencies sideband separating fundamental SIS mixers have been employed for example in ALMA [8], where a generic dual sideband (2SB) topology is used through out most of the bands reaching image rejections better then 10 dB. In this case the noise of the image band is rejected improving the sensitivity of the instrument. When it comes to submillimetre wave Schottky technology, the development of waveguide based 2SB receivers using either fundamental or subharmonic mixers has been nonexistent. However recently, as the STEAMR instrument, which is a part of the ESA PREMIER mission [5] intended for atmospheric observations, left the drawing board and entered a feasibility phase, the need for 2SB functionality has been addressed. The instrument baseline is a focal plane array of 14 heterodyne receivers operating in the 320 GHz to 360 GHz range, whereof 8 are to be 2SB with around 20 dB of image rejection. Since LO power comes to a high cost at submillimetre frequencies subharmonic mixers [29] are chosen as they have similar performance as fundamental mixers. The motivation for having SSB receivers is that for atmospheric observations typically a combination of many and broad spectral lines originating in both sidebands (the effect of line broadening is typically seen at lower altitudes at which the atmospheric pressure is higher) can be observed, see Fig. 1.1. To be able to resolve the individual lines a sideband separating topology becomes desirable. The instantaneous IF bandwidth for the STEAMR instrument is around 15 GHz. For traditional radiometric instruments that uses only one or a few DSB receivers, a modular approach i.e. using individual waveguide packaged mixers, multipliers and

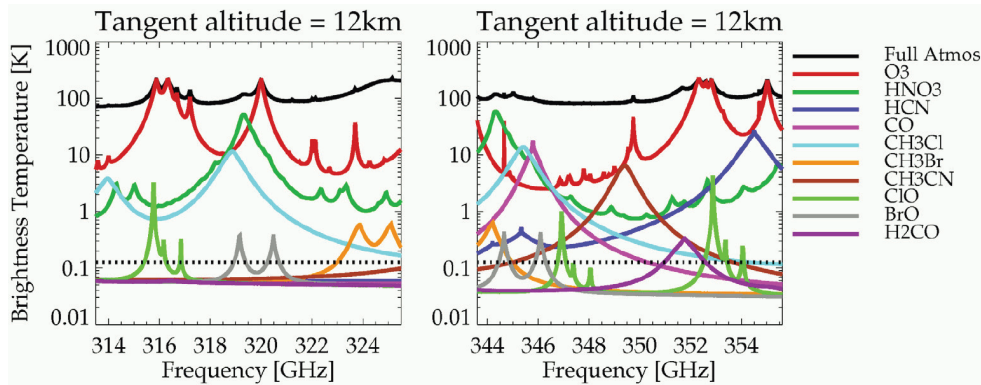


Fig. 1.1: Simulated frequency spectrum of the atmosphere at 12 km altitude as observed by the STEAMR microwave limb-sounder, ESA [5] - courtesy of D. Gerber.

coaxial packaged LNA's, would have been sufficient and most cost efficient. The integration and/or custom design of front-end components is mainly motivated as new and higher standards are set for radiometric instruments, as the system performance can be improved by the integration of components and by sharing and controlling mechanical and electrical resources. Naturally there are trade offs when choosing integration level, variability of components and yield are two limiting factors to consider.

Based on previous radiometer development at submillimetre frequencies at Omnisys Instruments AB, a 2SB submillimeter wave topology for subharmonic mixers was proposed to the Swedish Research Council (VR) for this research project. The proposed topology consisted of a 45-degree LO phase shifter hybrid and a matched Y-junction for the RF feed, compare to the work on subharmonic IQ-mixers [30] [31] and the development of a novel sideband separating SIS mixer [32]. The main outline for realisation of this novel concept at submillimetre wave frequencies is partially presented in Paper [A] with the main results of the full realisation presented in Paper [D]. In addition, initiated as a collaboration project with Rutherford Appleton Laboratories, a parallel development and demonstration of the proposed subharmonic sideband separating mixer topology has been conducted [33]. The advantage of using a matched Y-junction or the equivalent double E-plane probe design [34] for the RF, is mainly the larger RF bandwidth, low losses and ease of fabrication. However potential problems of this topology, such as RF standing waves from mismatches and generated mixer RF noise at the output, which are due to the poor isolation between the mixer RF ports, have to be considered, as they will for instance lead to large ripples in the image rejection response. This has led to the develop-

ment of an alternative and completely new topology, Paper [D-E], where a concept employing 90-degree LO and RF hybrids is proposed, leading to a considerable improvement in isolation between both RF and LO ports. In addition, this feeding arrangements reduces the LO and RF voltage standing wave ratio (VSWR) to a minimum, as ideally any reflections at the LO and RF ports are terminated in the isolated 4:th arm of the coupler. This reduces the effects of RF mismatches seen in the conversion loss response and leads to a more stable and broadband frequency response in general.

In this thesis the design and characterisation of a sideband separating (2SB) low VSWR subharmonic ($\times 2$) GaAs Schottky barrier diode mixer with integrated IF LNA MMIC's is presented. It is comprised of a 340 GHz IQ mixer that in addition with an IF quadrature hybrid alternatively with an IQ-IF spectrometer back-end makes it possible for the separation of the upper and lower sidebands. As a side result two novel differential phase shifter topologies are proposed suitable for planar integration giving an alternative to traditional waveguide based phase shifter hybrid solutions, Paper [B]. A novel approach for characterisation of submillimetre devices and circuits is also presented using waveguide embedded TRL-calibration integrated on THz membrane circuits, Paper [C]. Finally, in Paper [F] a short summary of the ALMA Water Vapor Radiometer (WVR) development is presented, in which I have mainly been involved in the design of the LO multiplier chain and design of the IF filter bank.

Chapter 2

Radiometer systems

A Radiometer is a sensor that can detect radio waves (electromagnetic radiation) in a certain frequency band. In atmospheric science the received signal is most often generated by thermal radiation from the object observed. The receiver subsystem is responsible for detection and quantification of the electromagnetic radiation. A summary of receiver DSB noise comparing different technologies is plotted in Fig. 2.1.

There are many different types of radiometers [26], e.g. the total power, Dicke, noise injection and correlation radiometer to mention the most common ones. The choice of receiver technology and design will differ depending on the application. For atmospheric spectroscopy the Dicke switch type calibration, which uses a reference load at the radiometer input for calibration of the received power at the antenna, is commonly used. The calibration method can compensate to a large degree for the system drift and instabilities and is relatively easily implemented. For space-borne applications the reference loads used for Dicke switching could be cold space ($T \approx 2.7$ K) or/and thermally stabilised loads onboard the satellite. For resolving characteristics of narrow molecular lines, spectral resolution in the order of MHz are needed. In such applications heterodyne detectors with high resolution back-end spectrometers are used. A schematic of a general Dicke switch radiometer system based on a heterodyne receiver is sketched in Fig. 2.2.

When it comes to Schottky receiver technology, whenever the sensitivity is good enough for the specific application, the relative simple realisation and low cost of Schottky based receivers make them a natural choice. Some characteristics of state-of-the-art THz submillimeter wave Schottky diode based receivers are:

- large instantaneous IF bandwidth ($B > 20$ GHz)

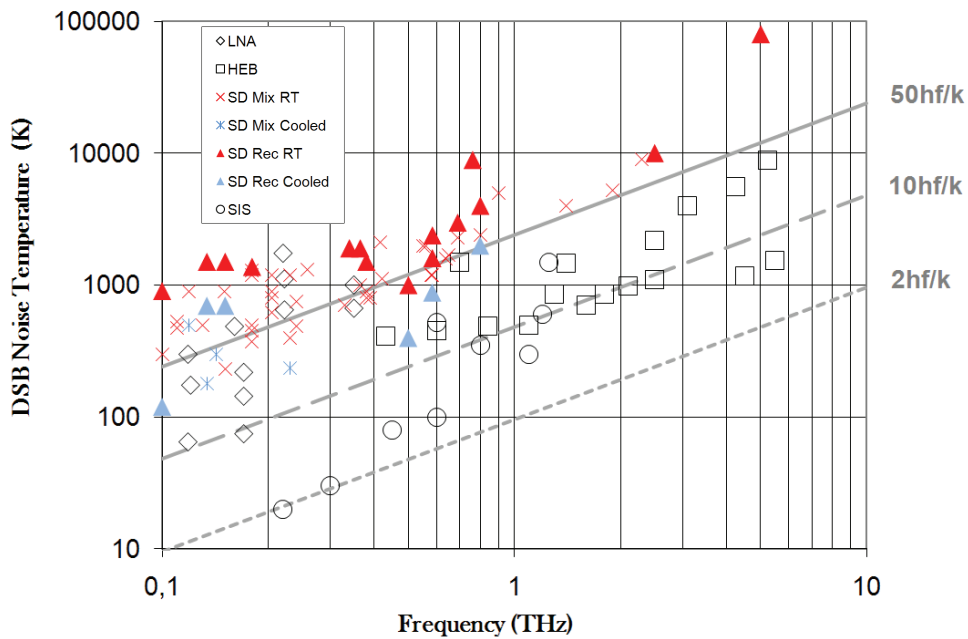


Fig. 2.1: Comparison of equivalent input DSB noise temperature results for various receiver technologies; cooled and room temperature Schottky diode mixers and receivers [19,35–57], HEB receivers [57,58], SIS receivers [57] and various LNA's [59–64].

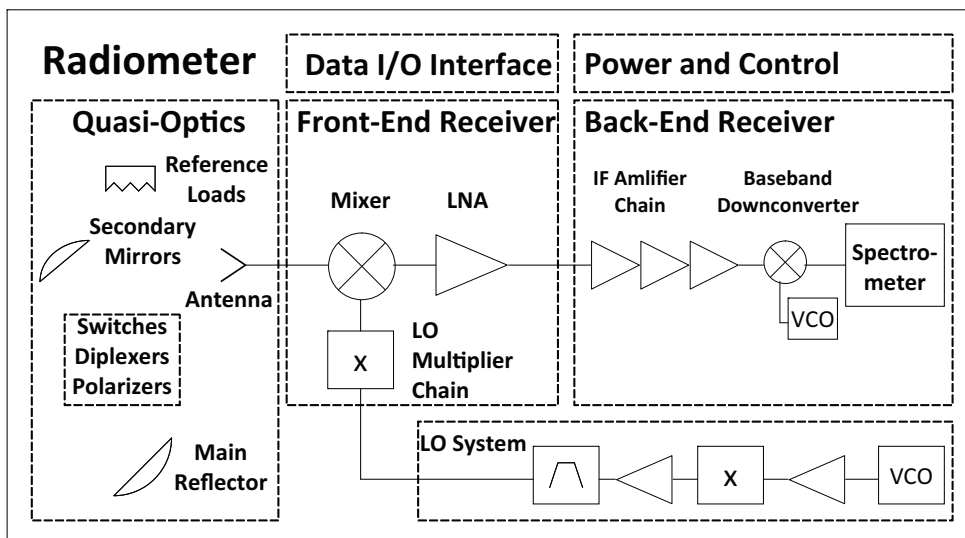


Fig. 2.2: Schematic of a Schottky based radiometer system.

- LO power (\sim mW)
- sensitivity $T_{rec,dsb}$ (\sim 1000 K to 10000 K)
- are waveguide packaged and use horn antennas

The level of LO power that is required for efficient pumping of the mixer diodes can be reduced to some extent by proper circuit design, by applying a DC bias to the diode or by using low bandgap materials with lower turn on voltage. For Schottky based receivers in particular, subharmonic GaAs diode mixers have become very popular since they reduce the required LO pumping frequency by a factor of two or more. In fact most of the high performance GaAs Schottky based radiometers operating in the lower end of the submillimeter wave band, use subharmonic x2 mixers [29], which have a very little increase of mixer noise and conversion loss compared to higher order harmonic mixers. The total amount of power required for generating a LO signal at half the RF frequency could in this way be reduced by as much as a factor of 10 compared to receivers based on fundamental mixers, given the low efficiency of multipliers and that the LO chain power level has to be raised. The number of components and gain in the LO chain is also reduced increasing the stability and reliability of the system.

When looking at the design of the multiplier chain, components with high efficiency, broad bandwidth and high multiplication factor are desirable. As these requirements do not necessarily go hand in hand there are trade offs to consider. For the design of efficient and stable multiplier chains, it is necessary to optimise each multiplier stage for the specific power level and frequency at which it will operate. Another important thing to consider is of course the availability of high power amplifiers for pumping the multiplier chain. Active devices are typically more efficient and are therefore used at the highest possible frequency. Various Schottky based doubler and tripler designs up to a couple of THz have been reported, [18]. Output powers exceeding 1 mW around 1 THz, sufficient to pump a Schottky mixer, have been demonstrated using power combining techniques. Another interesting alternative is the HBV diode [65], which has an inherent antiparallel IV and CV characteristic suitable for high frequency high power odd harmonic generation.

Heterodyne systems employing Schottky diode mixers are often used at submillimeter wave frequencies, because the signal phase information is preserved compared to direct detection, and because submillimetre LNA technology is not yet an option. For such systems the mixer and

IF LNA are responsible for the larger part of the receiver noise contribution. The receiver equivalent input SSB noise temperature, assuming no RF loss, can then be written as

$$T_{rec,ssb} = T_{mix,ssb} + L_{mix} \cdot T_{lna} \quad (2.1)$$

Thus, reducing the mixer noise $T_{mix,ssb}$ is equally important as reducing the product of the mixer conversion loss L_{mix} and LNA equivalent input noise temperature T_{lna} . Moreover, minimising RF input losses and mixer IF losses is also important as these will effectively increase the receiver conversion loss but also contribute with extra noise.

Another characteristic of Schottky mixers is the high impedance at the IF port, which is typically in the range of 100 Ohm to 300 Ohm. The IF mismatch between the mixer and LNA leads to a ripple response, which limits the radiometer performance. Specially for applications which require large IF bandwidths, this can become a problem, why the integration and co-design of a LNA and mixer must be considered. Instead of using impedance transformers or matching networks in general, which can be considered as relatively narrow band and introduce additional losses, a better way would be to custom design the LNA for a high input impedance and place it in the same housing as the mixer with minimum separation distance.

Chapter 3

Diode mixers

In this chapter some basic theory of Schottky barrier diode mixers is discussed with focus on the important tradeoffs between device parameters of modern high-speed Schottky devices. In figure Fig. 3.1 an example of a fuzed quartz mixer circuit and antiparallel GaAs Schottky diode can be seen.

3.1 Mixer theory

A mixer converts power from one frequency to another keeping the signal information intact by intermodulation with an LO signal. For a downconverting mixer the input high frequency RF signal is downconverted to a low frequency IF signal, see Fig. 3.2. The mixer efficiency is measured as the ratio of input and output power and is defined as the mixer conversion loss:

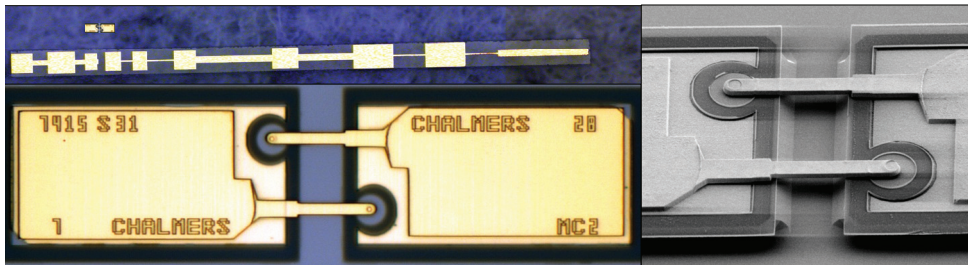


Fig. 3.1: Manufactured circuits and devices at Chalmers University of Technology. Fuzed quartz mixer circuit side by side with diode chip (top left), microscopic photo of an antiparallel diode chip (bottom left) and a SEM image of a similar device (right).

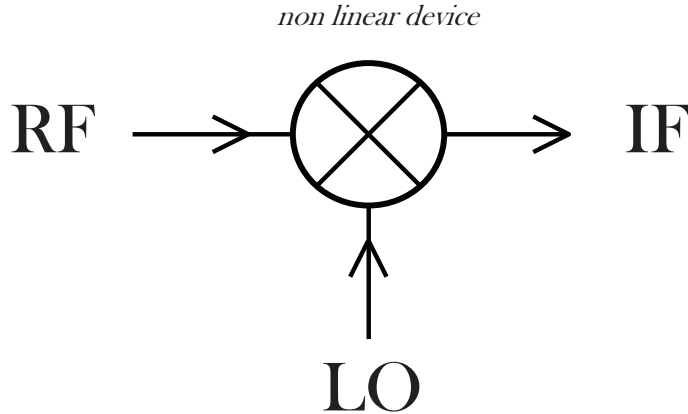


Fig. 3.2: Principle circuit schematic of a mixer.

$$L_{mix} = \frac{P_{RF,in}}{P_{IF,out}} \quad (3.1)$$

In resistive diode mixers it is the non-linear voltage-current characteristic that is used for frequency mixing. A resistive switch, variable from zero Ohms to infinity, makes a good first approximation of a resistive diode mixer. It has a theoretical conversion loss of -6 to -3.9 dB assuming a sinusoidal to square waveform [66].

In this analysis, the degradation factor of the conversion efficiency, due to non ideal switching in the real case, is found as the square of the difference between the maximum and minimum reflection coefficient for the two switching states, and is estimated to about 1 dB. The effect of mismatch losses contribute to an additional loss of about 1 dB. By this very simple analysis values of the intrinsic mixer conversion loss not far from simulated values of diode mixers, are obtained.

For Schottky diode mixers, degradation of the conversion efficiency is mainly due to the series resistance R_s and parasitic capacitance. In [67, 68] an analysis is made of this additional parasitic conversion loss, for finding the important trade offs in diode parameters for optimum performance at submillimetre wavelengths, predicting a minimum parasitic conversion loss contribution of 1 dB at 300 GHz to 4 dB at 1.5 THz.

Mixer conversion loss and equivalent input noise are the two main figure-of-merits that are used for characterisation of the mixer performance. For submillimetre wave applications the lack of efficient and powerful LO sources, makes optimisation of the of required mixer LO power important. Other important parameters are the RF, LO and IF

impedances, as well as conversion loss flatness and spurious generation. For image rejection mixers, IQ-mixers and sideband separating mixers (2SB mixers), the phase and amplitude unbalance or image rejection are significant. For high performance radiometer applications, high stability for accurate measurements is needed, why temperature drift effects etc. have to be considered.

The concept of using an antiparallel diode pair for subharmonic mixing, was proposed by Cohn in 1975 [29], with a performance similar to fundamental mixers. The antisymmetric IV-relationship of an antiparallel diode pair has an intrinsic suppression of even harmonics when pumped by a LO signal. As the diode pair conducts current in opposite directions for the positive and negative periods of an applied sinusoidal LO voltage, the effective differential conductance versus applied voltage becomes an even function (symmetrical). This results in a conductance time domain waveform with half the period compared to the applied LO signal, which is the fundamental principle behind subharmonic intermodulation. Depending on circuit design any even order harmonic of the LO can be utilised for downconversion, and for an ideal perfectly balanced diode pair only odd order LO harmonics will be generated outside the diode loop. In the same way currents containing the even harmonics are confined in the diode loop and canceled outside the diode circuit. The most common mixer type is the subharmonic (x2) mixer also referred to simply as a subharmonic mixer, which utilises the second harmonic of the LO signal for downconversion of the RF signal.

3.2 Schottky diodes

The name Schottky diode has been awarded Walter Schottky for his pioneering work during the 1930's and 40's in the field of metal-semiconductor interfaces [69]. However the discovery of the rectifying effect of a metal to semiconductor transition goes as far back as to 1894 and experiments conducted by Ferdinand Braun on metal-sulfides [70]. The Schottky-barrier model proposed by Cowley and Sze [71, 72], explains most of the characteristic phenomenons seen in Schottky rectifiers. It includes the effects of surface states in the metal-semiconductor junctions, first pointed out by Bardeen [73], and the effect of image-force lowering of the barrier, also known as the Schottky effect, which is more pronounced in the backward biasing direction.

The main responsible forward current transport mechanism at room temperature is thermionic emission. By applying a positive forward voltage (positive at metal interface), leading to a positive offset of the thermal energy of electrons in the conduction band relative to the metal, we allow for the transport of electrons over the barrier and into the metal

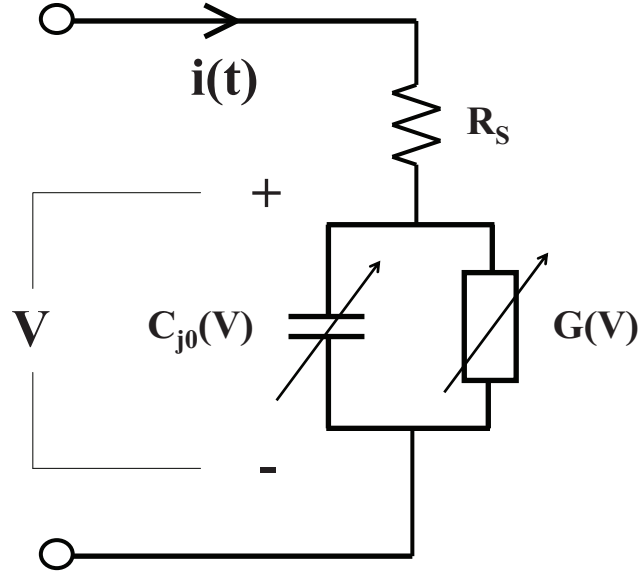


Fig. 3.3: Electrical model of diode.

contact. The exponential dependence of the electron distribution, gives the non-linear relationship between the forward current and applied voltage:

$$I(V) = I_S (e^{\frac{q(V - IR_s)}{\eta k_B T}} - 1) \quad (3.2)$$

with I_S being the reverse saturation current, R_s the series resistance, η the diode ideality factor, k_B the Boltzmann constant and T the temperature.

The Schottky diode is a majority carrier device and does not suffer from the slow recombination processes of PN junctions. Furthermore it can be designed with minimum parasitics owing to its simple 2-port structure (metal-semiconductor junction). The Schottky diode is therefore well suited for high-speed operation with reported cut-off frequencies reaching several THz. The cut-off frequency is defined as:

$$f_c = \frac{1}{2\pi R_s C_{tot}} \quad (3.3)$$

with C_{tot} being the diode chip total capacitance. The rule of thumb is to have a cut-off frequency ten times higher than the operating frequency. However, the cut-off frequency does not give a measure on the conversion efficiency, bandwidth or noise. That is why the device parameters R_s , C_{j0} , η and C_{tot} are used instead as they are relatively few and give a more direct measure of the expected device performance. In Fig. 3.3 an electrical circuit representation of the diode is shown.

Optimisation of the Schottky barrier and parasitics is crucial for submillimetre frequency operation. Epilayer thickness, doping concentration, contact size and layout have to be optimised. In general the epilayer thickness is chosen to be around one zero bias depletion width, as to large thickness will only add to the resistance. The doping concentration for high frequency diodes is chosen rather high, in order to reduce the series resistance coming from the undepleted region of the epilayer and to reduce hot electron effects, but without increasing the tunneling effects and leakage current to much. As the resistance increases and the junction capacitance decreases with smaller anode size, there is a trade off in between these two parameters influencing the diode cut-off frequency, bandwidth and noise. In other words, THz diodes have to be small enough to eliminate parasitic losses due to the junction capacitance keeping the series resistance at a minimum to reduce the conversion losses and noise.

When it comes to the structure of modern THz Schottky diodes used for THz detectors and sources, planar devices are preferred to whisker contacted devices owing to their ability to withstand stresses and the superior repeatability. The assembly of planar devices is also less challenging. Moreover, complex diode structures such as antiparallel, antiseriess and in-series diode configurations found in subharmonic mixers, balanced mixers and multipliers are only possible thanks to planar technology. For the diode chip design, trade offs also exist. The most important is between pad capacitance, finger inductance and finger capacitance [74], which influence the device performance. A lumped model of a antiparallel diode and its 3D correspondence is shown in Fig. 3.4. Device modeling and parameter extraction requires some kind of lumped device model. The lumped model is important for optimisation and design of a device structure to be able to understand the various parasitic contributions. When functional it can to a large extent replace tedious 3D-EM simulations.

3.3 Noise theory

There are three mechanisms that mainly contribute to the diode intrinsic noise. These are the shot noise, thermal noise and hot electron noise [76].

The shot noise comes from the discrete nature of the non-linear current mechanism of the diode and is due to random variations of the electrons passing through the barrier.

Thermal noise (also called Johnson or Nyquist noise) is due to the diodes series resistance and is together with shot noise a major noise contributor in room temperature applications.

Hot electron noise (hot noise) or high field noise, which is due to a non-equilibrium distribution of electrons in the conduction band and

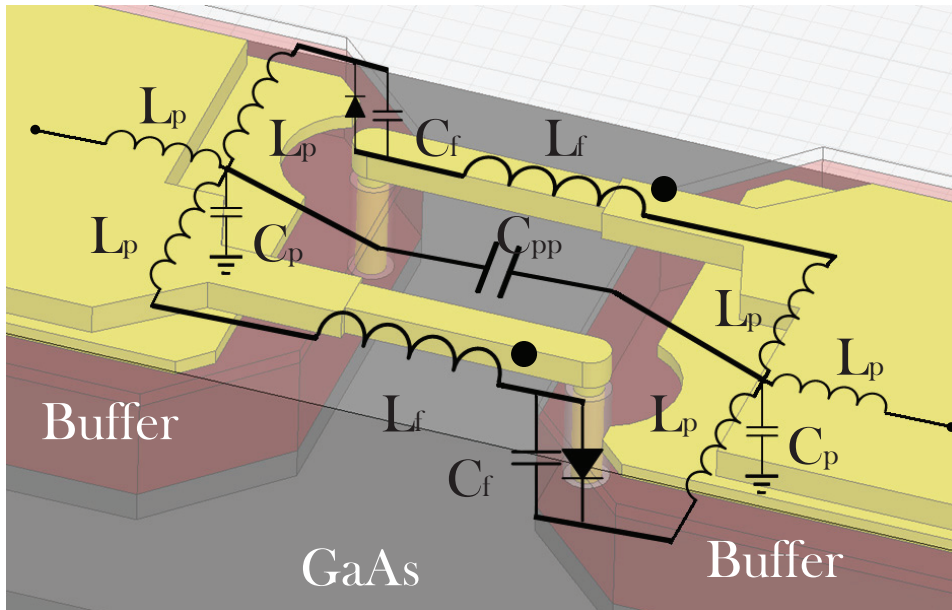


Fig. 3.4: Lumped model of the anti-parallel planar diode with mutual inductive coupling between fingers [75] on top of a 3D-model with coaxial ports

scattering effects, will come in to effect at high current distributions and voltages.

When cooling a diode, the thermal noise contribution will decrease and the effects of shot noise will start to dominate, this is why we say that the cooled Schottky diode is shot noise limited. For high frequency resistive mode operation the parasitic junction capacitance parallel with the barrier has to be reduced for efficient coupling of power to the diode. The consequence, as stated earlier, is that smaller devices have to be used leading to an increase in series resistance, since it is inversely proportional to the contact area and contact circumference. The series resistance will also increase due to the skin effect. Overpumping diodes leads to strong current densities in the barrier causing an increase in the total noise that is due to hot electron noise, mainly coming from different scattering effects. Applying a DC bias would also increase the noise as the average current density is increased. A general noise model adopting the effects of thermal, shot noise and hot noise contributions, can be used [77] for accurate prediction of mixer noise.

Chapter 4

Design of subharmonic mixer

This chapter deals with the general aspects of basic waveguide coupled circuit designs. The emphasis is on the design of a subharmonic $\times 2$ mixer employing antiparallell diodes, for which a "divide and conquer" design approach has been adopted, breaking up and identifying the various circuit parts and allowing for a systematic design approach, see Fig. 4.1. Moreover ideal to full 3D simulations have been compared, pointing out the importance of 3D modeling to more accurately include the effects of device parasitics. Finally considerations of the 2SB mixer design are presented.

The design process flow, seen in Fig. 4.1, starts by definition of the topology and is then divided into separate parts that can be designed independently. These designs are then combined one by one and a co-optimisation is done.

4.1 Circuit technology considerations

The choice of circuit technology is important and mainly decided by the technologies that are at hand. Submillimetre wave circuit implementations ranges from the simpler low frequency hybrid circuits, that use quartz carriers and flip chip mounted discrete diodes, to high frequency membrane MIC with an arsenal of circuit features such as beamleads, on chip resistors and capacitors. In between we find circuit technology hybrids such as quartz circuit carriers with beamleads and/or with integrated active components using substrate transfer techniques, and custom MIC's with integrated waveguide probes, that have been thinned down to extreme thicknesses.

The choice of circuit technology will influence and limit the number of choices for the circuit topology. For waveguide packaged mixers, which are considered here, the machining capabilities will also influence the choice of topology as waveguide components and waveguide to circuit transitions are vital parts of the design. For this particular mixer

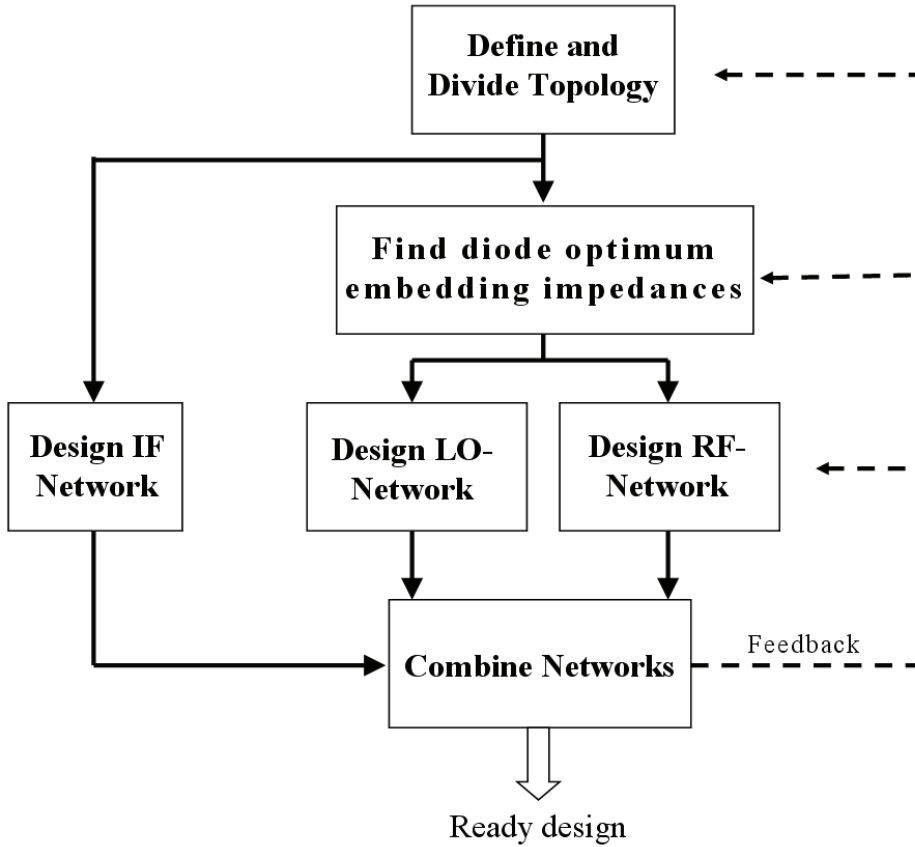


Fig. 4.1: Mixer design process flow chart.

design the goal was to use circuits that can be fabricated commercially, why a hybrid circuit design using a quartz carrier and a discrete diode chip was chosen. Hybrid circuits using ultra thin quartz substrates and discrete anti parallel diode chips that are soldered up side down (flip-chip mounted) on to the quartz carrier, have been reported up to about 600 GHz. It is also the highest frequency for which discrete commercial diodes are available [78].

To minimise the number of critical assembly steps and maximise repeatability of the circuit assembly a suspended inverted mixer topology was chosen, similar to [40]. To be able to use commercially available circuit fabrication processes and for the substrate to be able to withstand stresses due to the extremely long circuit dimensions (~ 5 mm) of the design compared to the thickness (~ 75 μm) and width (~ 240 μm), the substrate thickness was maximised. Furthermore, as this topology optimally requires reduced height waveguides, both for the RF and LO, it sets slightly tougher requirement on the machining capabilities com-

pared to full height waveguide mixer designs.

4.2 Subharmonic (x2) mixer topologies

Efficient subharmonic intermodulation can be achieved using a single diode, by designing idlers at the undesired multiples of the LO frequencies. However difficulties in separating the RF signal from the LO has lead to the development of the more common antiparallel diode topology which inherently suppresses even harmonics.

The subharmonic x2 mixer uses half the effective LO frequency giving almost the same conversion efficiency and noise as fundamental single ended diode mixers. It also gives a natural separation of the RF and LO ports that simplifies the circuit design considerably. An antiparallel diode configuration can be implemented either in a series circuit configuration or in a shunt circuit configuration to ground. The main difference of these two topologies is that the blocking filters have to provide a short circuit in one case and an open circuit in the other, see Fig. 4.2.

The antiparallell chip is more suitable for high frequency operation as its circuit realisation is much simpler then for the diode series pair, which requires a ground connection for the diodes. The diode series pair configuration becomes interesting for THz Monolithic Integrated Circuits (TMIC) designs, which allow realisation of more complicated circuit structures and possibility to individually bias the diodes [79].

4.3 E-field coupled rectangular waveguide to planar transmission line transitions

The purpose of the waveguide probe is to efficiently couple power from the planar transmission line mode to the rectangular waveguide mode. In this context we only consider the specific case of probes coupling to the fundamental TE₁₀ mode of rectangular waveguides with a 2:1 ratio. Supporting only one polarization this is by far the most common waveguide type used in submillimetre wave mixer applications. We also consider the case in which the transmission line is situated on a substrate inside a shielded channel. The mode of the planar transmission line is either in microstrip, suspended stripline, CPW or a combination thereof, as the tightly shielded environment will lead to coupling to the surrounding ground walls. Even under such limitations numerous types of waveguide probes are possible to design. The transmission line plane can be oriented in or perpendicular to the E-plane of the waveguide mode. The choice will have an influence on how the mechanics are to be machined, possibility to integrate other waveguide components

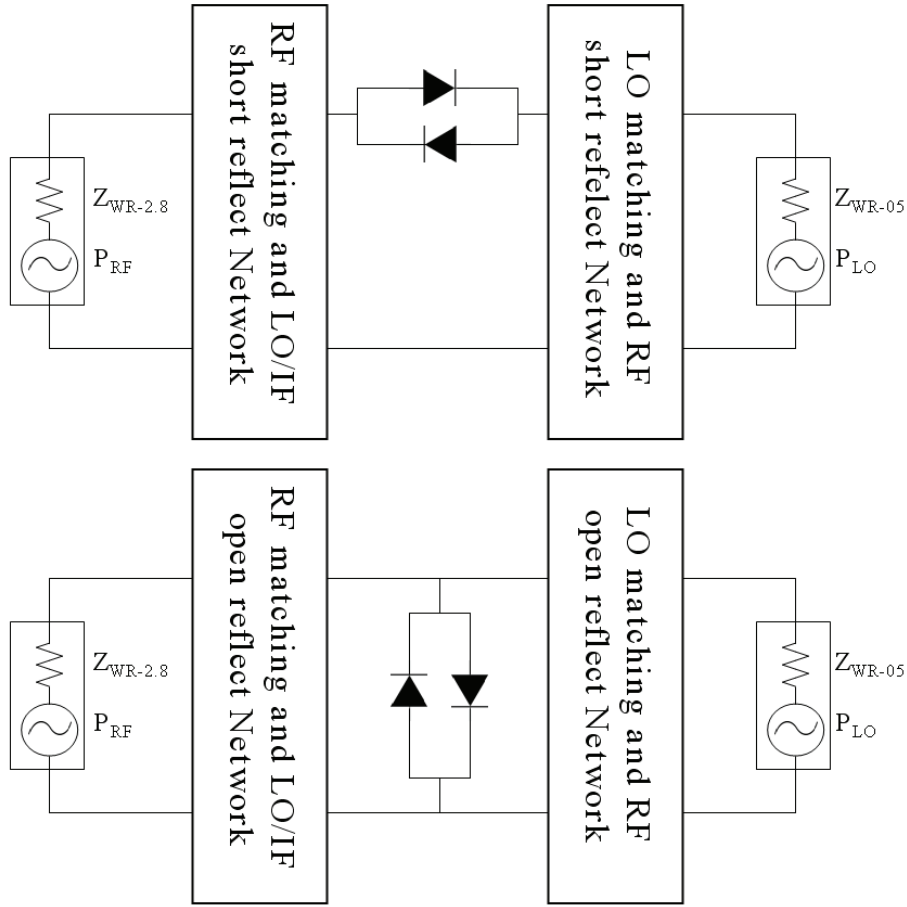


Fig. 4.2: Schematic of series (top) and shunt (bottom) type mixer topologies employing antiparallel diodes.

and assembly cavities to the same block. It will also affect the probe response, in terms of bandwidth and matching properties and the physical shape of the probe design. In our case we consider E-plane type splitblocks, which are typically used for broadband high frequency and low loss applications, as the current of the waveguide mode is propagating along the split and not across it.

When deciding on the probe functionality, the simplest case is when no additional functionality is needed, that is a single E-field probe with a waveguide backshort. If a ground connection is needed a planar backshort can be used similar to the mixer design RF probe seen in Fig. 4.8. The transmission line backshort can be replaced by a RF choke filter providing an alternative path at lower frequencies, see Fig. 4.6. Full height waveguides or reduced height waveguide with broader frequency response can be used. Reduced height waveguides are however more

difficult to fabricate, as they require larger aspect ratios of the cutting tool. The use of reduced height waveguides can also provide additional tuning functionality when the probe is a part of a matching circuit or when matching is done in the waveguide, and is commonly used in various waveguide based circuit designs.

By putting an additional probe in the same plane as the single E-field probe, but on the opposite side of the waveguide a balanced dual probe design can be made with the two probe feeds being 180 degree out of phase [34]. It is also possible to design differential (balanced) line probes [80,81], with a single launch entering the short length side of the waveguide. For doubler designs a crossbar type topology is very common, having the active components integrated with the waveguide probe. This topology features a center feed at the end of the waveguide backshort which is isolated from the fundamental waveguide mode. Another differential probe that also is launched at the back short end of the waveguide uses a dipole antenna for coupling to the waveguide mode [82]. It is also possible to utilise a tapered ridged waveguide structure for transformation from a microstrip type mode to the TE₁₀ waveguide mode [83].

4.4 Planar filter structures

The most commonly used planar submillimetre wave filter is probably the RF choke filter with alternating low and high impedance quarter wavelength long sections, see Fig. 4.6 and Fig. 4.7. This filter topology offers a very good rejection to a relative few number of sections. The main advantage of using it is that for hybrid circuits the same substrate is also used for coupling to the waveguide mode, which requires an effective substrate/mounting channel width below cutoff. This gives very little or no space for the realisation of open stubs. A less common alternative is to use the more complex hammerhead filter topology or curved open stubs.

Electrical shorts require some kind of grounding mechanism i.e. plated vias or beamleads, for this advanced processing is however required. Traditional bondwires are too large in size and are too inaccurate to be used. An alternative is to use gold wires soldered to the block and to the circuit in a similar fashion as the soldering of the diode chip, however this is not advantageous from a repeatability and production perspective. Therefore filter topologies requiring electrical ground are avoided as much as possible.

The best way in terms of reproducibility and ease of assembly of grounding the circuit is by using beamleads that are clamped in be-

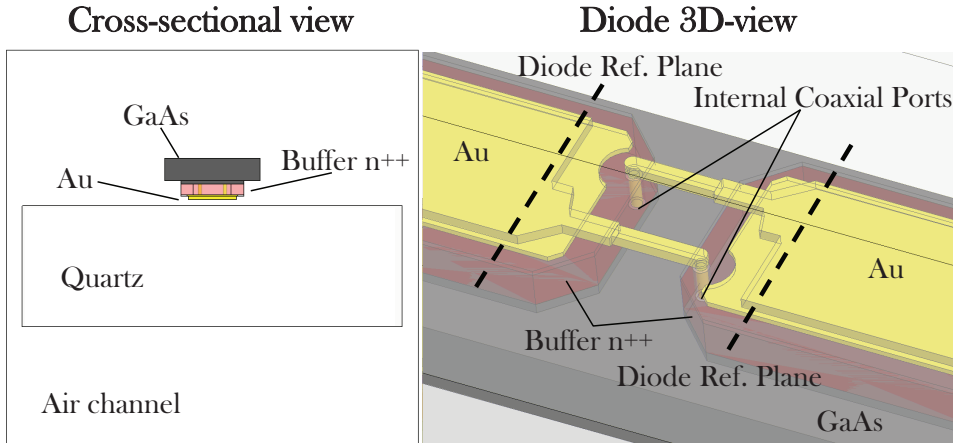


Fig. 4.3: Full 3D-Model used for EM simulation of the flip-chip mounted antiparallel diode chip.

tween the two split blocks. Beamlead manufacturing requires a process in which the substrate carrier is etched away. Both quartz circuits and GaAs circuits can be manufactured with beamleads by etching and/or lapping techniques. An alternative to beamleads is to suspend the substrate in an inverted position, in which the suspension points can be used as ground connections to the block or as signal connections for low frequency or DC interfaces.

Coupled line filters are easily implemented and could give advantages in terms of bandwidth and better match. Multisection coupled line filters typically suffer from high transmission losses but also add directly to the total length of the circuit and are therefore avoided. On chip capacitors are mainly used for providing a DC connection for biasing working as AC ground.

4.5 3D-modeling of diode

To be able to accurately predict the diode chip optimum embedding impedances a full 3D EM simulation of the diode chip in its circuit environment is necessary, see Fig. 4.3. By replacing the active part of the diode with internal coaxial or lumped port [74], the diode non-linear part and passive circuit part can be combined, see Fig. 4.4. The diode pad interface has been extruded and the transmission line ports are later de-embedded back to the diode reference planes.

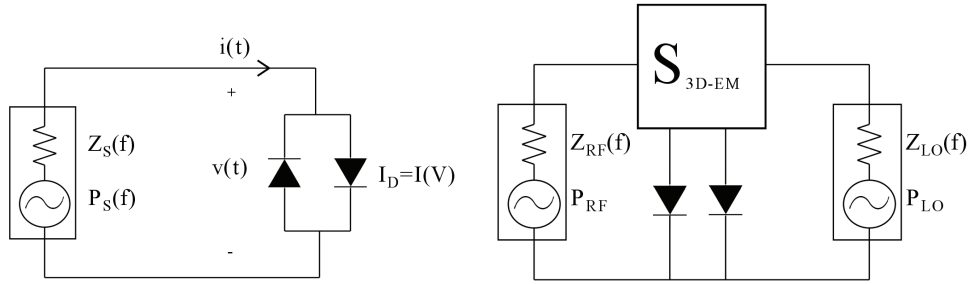


Fig. 4.4: Principle HB simulation setup of the antiparallel diode mixer topology, ideal case (left) and combining 3D-EM simulations of the diode chip.

4.6 Diode embedding impedances

By adding the influence of the chip parasitics, the optimum embedding impedances change dramatically compared to the ideal case. The 3D EM simulation of the diode chip with internal ports for the active components was imported in the form of a S-parameter file. The diode component was then connected to the internal ports and down to ground. Important is to consider the phase of the port and diode in order to get the antiparallel configuration right, see Fig. 4.4. By running harmonic balance simulations, the optimum conversion loss RF, LO and IF impedances can be found, see Fig. 4.5. The optimum noise and conversion loss points are assumed to be close one another, why the mixer design was mainly based on the conversion loss simulations, similar approach as in [74]. Idlers for the remaining frequency mixing products have to be used, and were in this case implemented by using a frequency dependent source impedance definition. Different simulation schemes, applying perfect ground (ideal), open or 10 Ohm (average real) for the termination of the mixing products, were used without any large impact on the optimum embedding impedances. The LO power level was found to be an important parameter for reaching convergence in the simulation. Another way to include the parasitics of the diode is by a lumped model, which can be based on 3D-EM modeling, and when complete offers a very efficient way of parameterised modeling and optimisation of the diode structure.

4.7 LO/IF filter circuit

Before starting on the more extensive LO and RF circuit design, it is a good idea to get acquainted with the waveguide circuit environment by investigating the design of the LO/IF duplex filter, see Fig. 4.6. This particular design can be divided into three parts, partial design of a

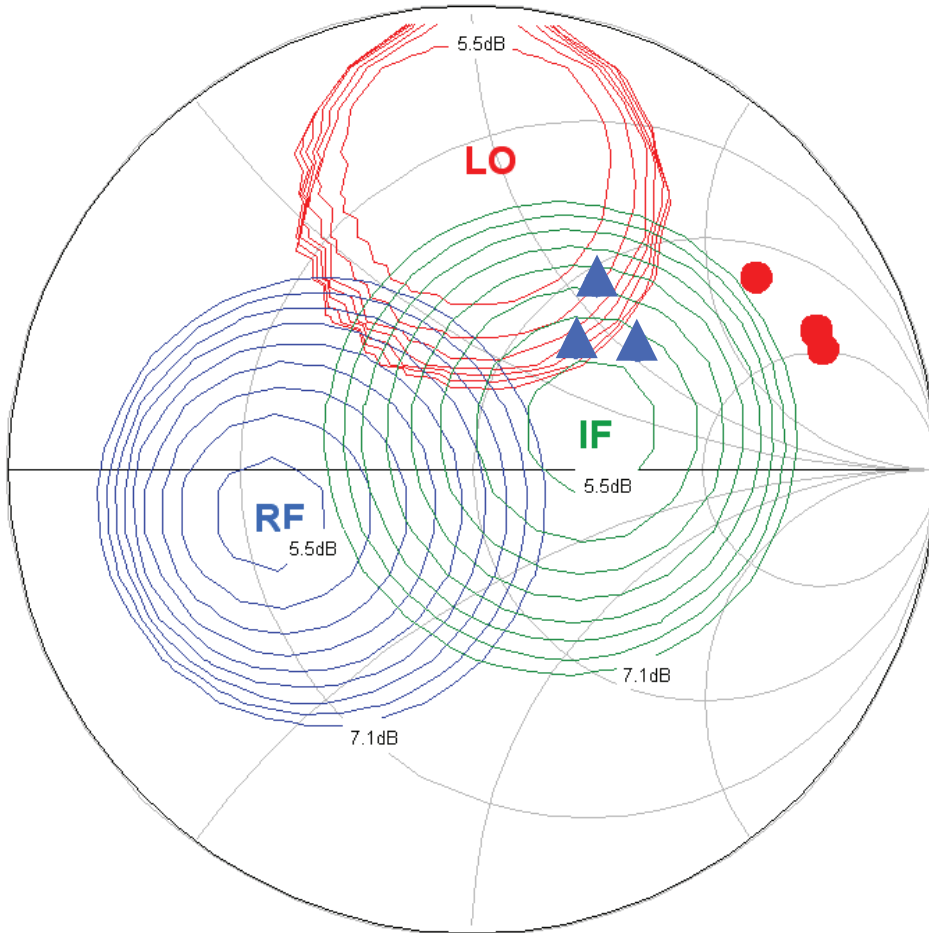


Fig. 4.5: Comparing HB simulated optimum RF (triangles) and LO (circles) conversion loss diode embedding impedances (compared with [40,74]) for $f_{LO} = 170$ GHz, $f_{RF} = 340$ GHz and $P_{LO} = 1$ dBm, for ideal antiparallel diodes using the VDI-SD1T7-D20 chip parameters with $R_s = 13$ $C_{j0} = 1.5$ and $\eta = 1.3$, and conversion loss contours from 5.5 dB to 7.1 dB in 0.2 dB steps for the VDI-SC1T2-D20 chip with $R_s = 8$, $C_{j0} = 3.5$ and $\eta = 1.2$, including 3D-EM modeling.

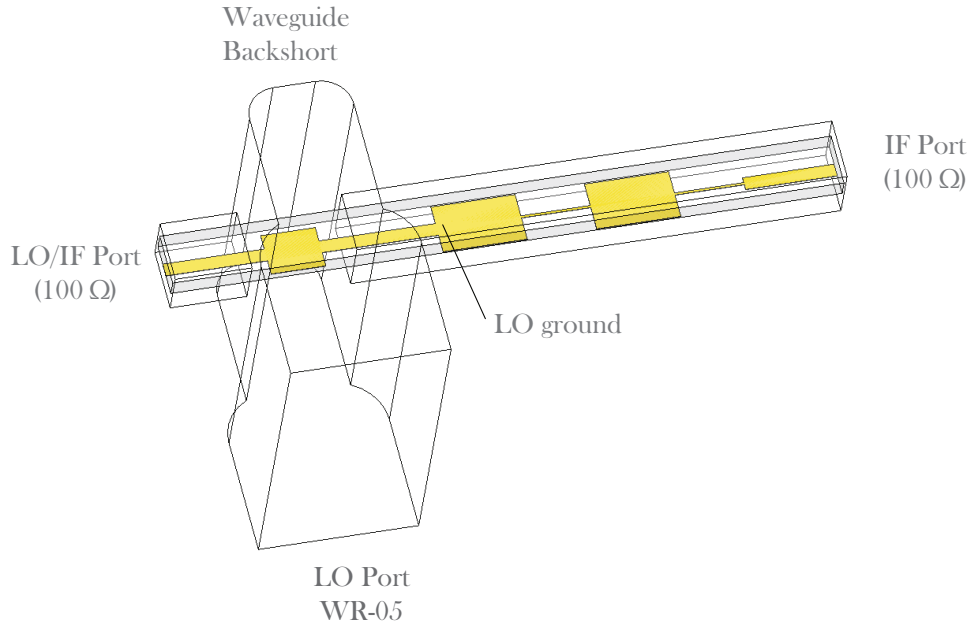


Fig. 4.6: Full 3D-Model used for EM simulation of the complete LO/IF duplex filter.

symmetrical LO probe (to WR-05), design of a planar LO stop filter, and final co-optimisation of the two. The harmonic balance simulations suggest an optimum IF impedance of above 100 Ohms, which was chosen as the characteristic impedance for the transmission line port interfaces. The characteristic impedance also has to give reasonable line widths for the low and high impedance filters and will effect the matching circuit design. Moreover a larger characteristic transmission line impedance, results in a smaller transformation ratio to the waveguide mode impedance (larger then 300 Ohms) simplifying the design of the waveguide probe.

4.8 LO matching circuit

Once the diode chip optimum embedding impedances are found the design of the matching circuits can start. The LO matching circuit should also work as an RF stop filter and provide a ground return for the RF signal at the diode. Different options for the realisation of the LO circuit exist. Important to consider is that the RF ground response will effect the RF bandwidth. For our application the LO absolute bandwidth is less then 5 GHz at 170 GHz which corresponds to about 3 %. The RF bandwidth is about 45 GHz at 340 GHz corresponding to more then 13 %. Therefore a RF choke filter topology with a low impedance section directly at the diode chip was chosen, as it gives the

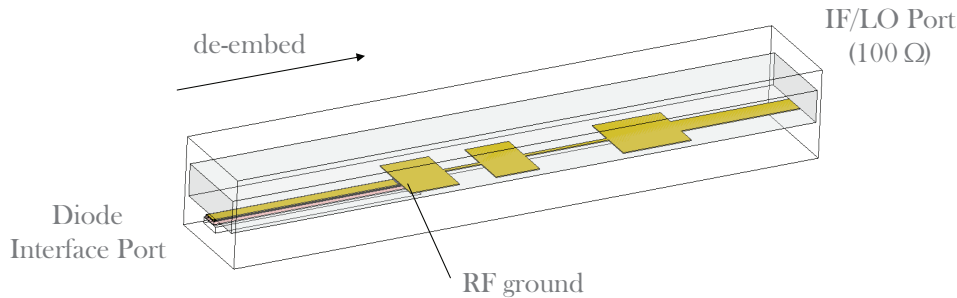


Fig. 4.7: Full 3D-Model used for EM simulation of the RF ground/ LO matching circuit.

most broadband RF response, see Fig. 4.7. The remaining sections were then optimised to maintain the broad RF ground response and give a sufficient match for the LO signal. The LO probe can also be utilised and be a part of the LO matching. The diode chip interface has been included in the simulation, in which the diode port is de-embedded to the correct diode reference position.

4.9 RF matching circuit

The RF matching circuit contains both planar circuitry, as the diode is positioned inside the mounting channel and a 3D waveguide part (WR-2.8) using a reduced height waveguide in the part where the RF coupling probe is positioned, see Fig. 4.8. Moreover a planar backshort on the other side of the waveguide is used for an IF ground return which also is transformed back through the RF probe and matching structure to a LO ground at the diode chip. The reduced height not only works as an extra matching section for the RF matching network, but also reduces the distance between the planar short and the diode chip which is required to be approximately half a wavelength at the LO frequency. The diode chip interface is also included in the simulation in which the diode port is de-embedded to the correct diode reference position.

4.10 Mixer circuit modeling

When all subcircuits have been optimised the complete mixer is simulated and final tweaks can be made, see Fig. 4.9. The S-parameters of this simulation can then be plugged into the HB-simulation. The designed matching circuits reflection coefficients are presented in Fig. 4.10 on top of the optimum conversion loss contours.

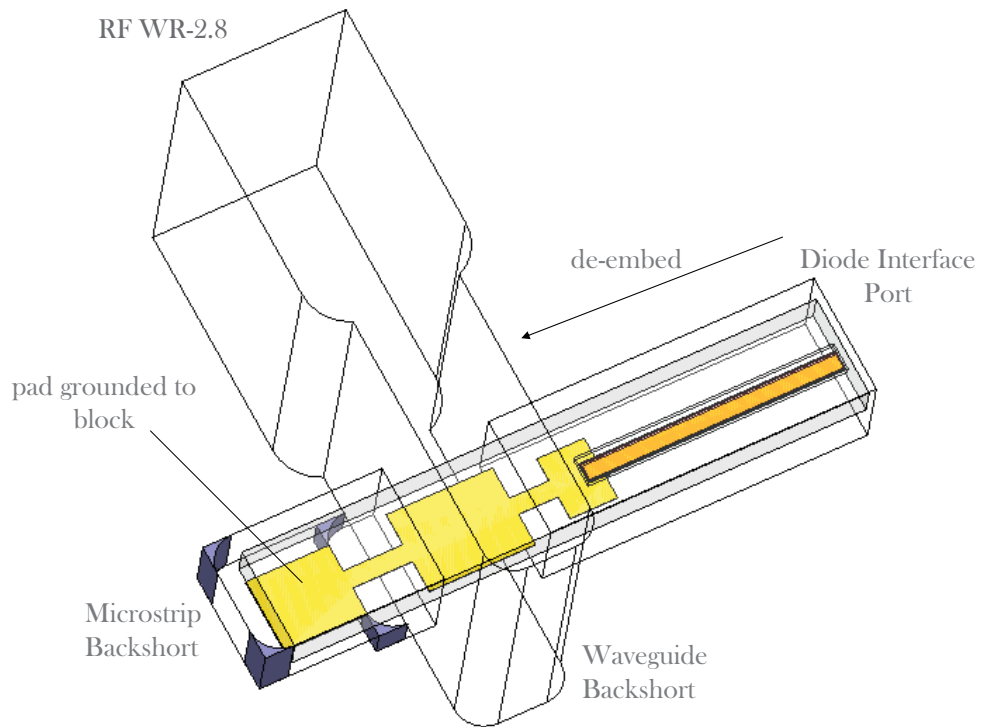


Fig. 4.8: Full 3D-Model used for EM simulation of the LO/IF ground/ RF matching circuit.

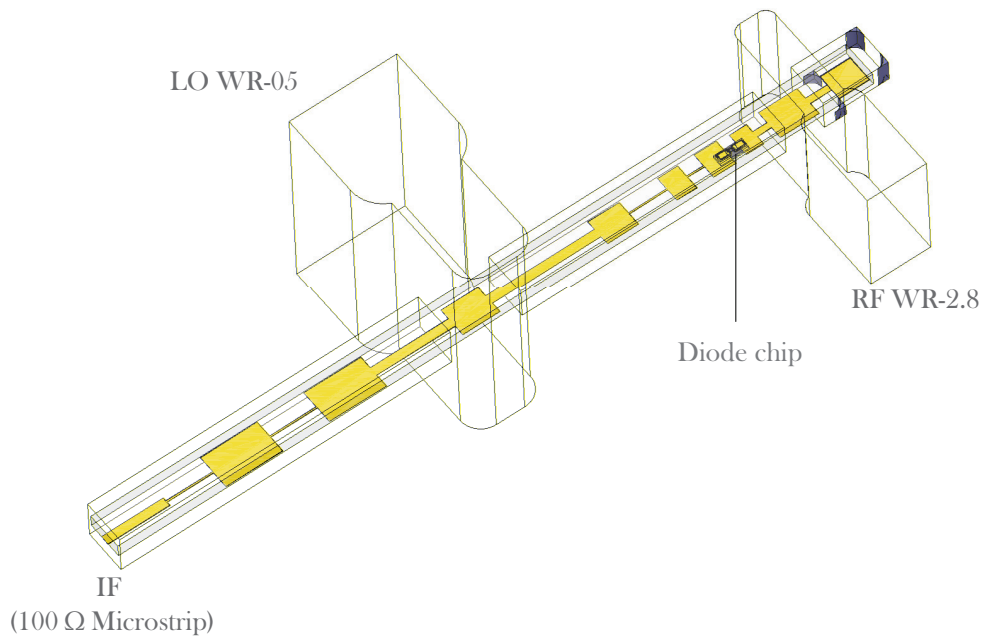


Fig. 4.9: Full 3D-Model used for EM simulation of the complete mixer design.

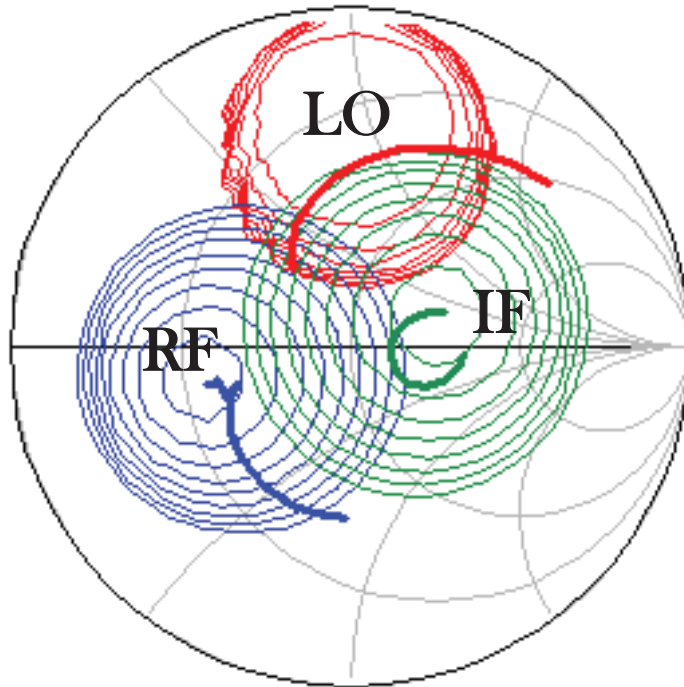


Fig. 4.10: Equivalent reflection coefficients of the RF and LO matching circuits seen from the diode reference plane for the RF, LO and IF frequencies.

4.11 2SB mixer design

Sideband separation (2SB) could be implemented using waveguide or quasioptical diplexers and image rejection filters [84]. These are however bulky, expensive and have little or no tunability in frequency. Moreover any losses in the RF path leading to the receiver will directly translate to an increase of the noise temperature. For these reasons a waveguide integrated sideband separating mixers approach was chosen, with relative low input losses and broadband frequency characteristics. Traditional waveguide components such as branch guide couplers and Y-matched waveguide junctions have been the building blocks considered for realisation of the mixer, as they are relatively easily implemented. By simple analysis of sideband separating subharmonic mixer topologies, with the effective LO phase difference being twice of the subharmonic LO hybrid, the following hybrid topologies are possible, see Fig. 4.11.

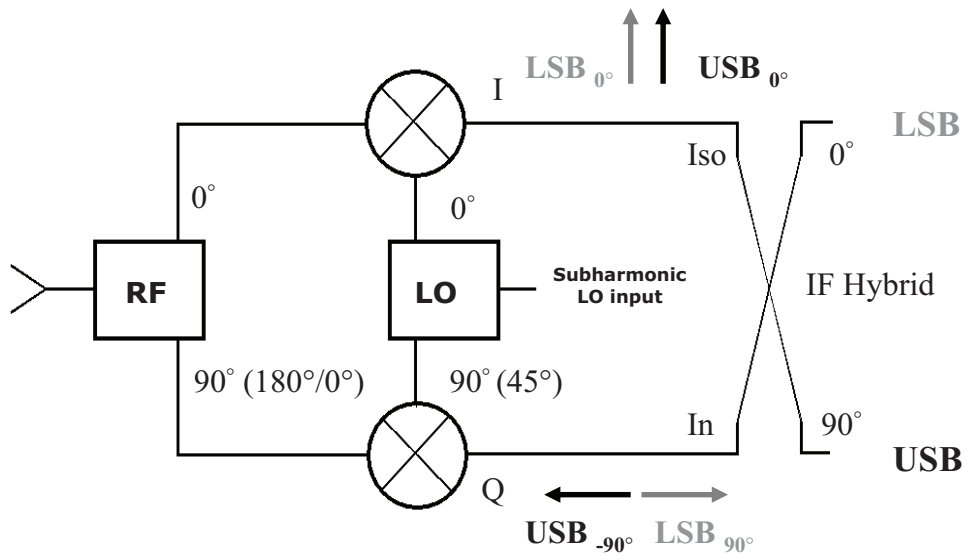


Fig. 4.11: Schematic of possible 2SB mixer configurations employing subharmonic mixers and various hybrid options.

Chapter 5

Characterisation of mixers

This chapter discusses Y-factor measurements in general and the different measurement setups that have been used for characterisation of the mixers that are presented.

5.1 Noise measurements

In this chapter the basic theory of Y-factor characterization of DSB mixers is briefly touched up on. Much of the analysis can be found in [76]. SSB Y-factor measurements are also possible but require measurements of the image rejection [85]. However, such measurements have not yet been conducted and are therefore left out in this discussion.

The Y-factor of the receiver system is measured using two reference loads at different temperatures, see Fig. 5.1. We used hot (RT *EccosorbTM* absorber, 290 K) and cold (*EccosorbTM* in liquid nitrogen, 77 K) load terminations coupling to a horn antenna connected to the mixer. The Y-factor is defined as the ratio between the measured hot and cold load noise power at the IF port. A power meter is connected via a YIG-filter (with a typical bandwidth around 50 MHz) to the output of a IF LNA chain, in order to get a good frequency resolution. For DSB mixers the radiation from the upper and lower sidebands will be added together at the downconverted IF band and therefore it has to be accounted for twice.

The total input noise power P_{tot} can be expressed as the sum of the noise power delivered by the load with equivalent noise temperature T_{load} to the antenna plus the equivalent receiver system input noise power and its equivalent receiver SSB input noise temperature $T_{rec.,ssb}$. The detected output power depends on the system gain G and bandwidth B (in this case defined by the YIG-filter), and can be written as:

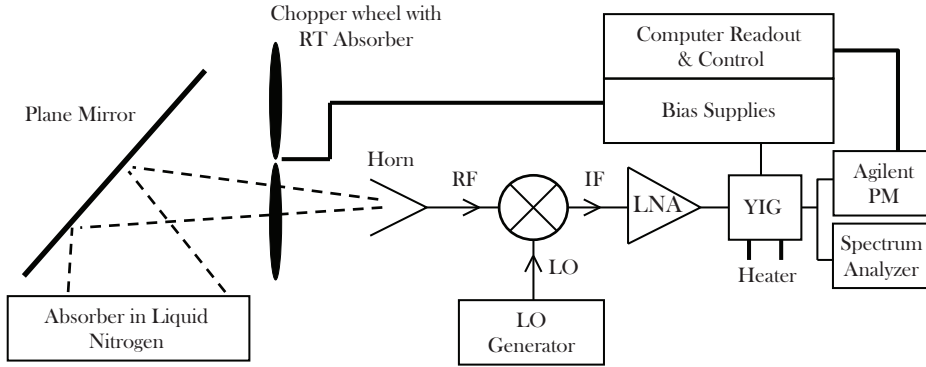


Fig. 5.1: Schematic of hot and cold load setup for Y-factor measurements.

$$P_{tot} = (T_{rec.,ssb} + 2 \cdot T_{load})G \cdot k_B \cdot B \quad (5.1)$$

with k_B being the Boltzmann constant. The Y-factor is then defined as:

$$Y \equiv \frac{P_{hot}}{P_{cold}} = \frac{(T_{rec.,ssb} + 2 \cdot T_{hot})G \cdot k_B \cdot B}{(T_{rec.,ssb} + 2 \cdot T_{cold})G \cdot k_B \cdot B} \quad (5.2)$$

We can see that the Y-factor which is the ratio in the received total hot to cold noise power, is independent of the unknown B and G parameters and only depends on the known hot and cold load temperatures T_{hot} and T_{cold} respectively, and the unknown receiver noise temperature. The generated noise power from the load, is coming in from both sidebands why there is a multiplication factor of two in front of the equivalent load temperature term. If we divide the numerator and denominator by two we get the equivalent expression for the receiver DSB noise temperature.

$$Y = \frac{(T_{rec.,dsb} + T_{hot})}{(T_{rec.,dsb} + T_{cold})} \quad (5.3)$$

In this analysis the upper and lower sidebands are assumed to contribute equally to the receiver noise temperature (in reality they differ and we have a sideband ratio to consider). The DSB noise temperature can then be defined as the total equivalent input noise temperature equally divided over each sideband. The SSB noise temperature is defined as the equivalent input noise temperature entering only from one sideband where the other sideband has no noise contribution, that is why the SSB noise is twice as high as the DSB noise. The important thing to keep in mind in the general confusion between the SSB and

Table 5.1: Receiver DSB noise temperature in Kelvin versus Y-factor in dB with $T_{hot}=300$ K (RT) and $T_{cold}=77$ K (LN)

Y [dB]	$T_{rec.,dsb}$ [K]	Y [dB]	$T_{rec.,dsb}$ [K]
0.1	9500	0.6	1430
0.2	4650	0.7	1200
0.3	3040	0.8	1030
0.4	2230	0.9	890
0.5	1750	1	780

DSB conventions, is that any continuum noise radiation seen by the receiver antenna enters the system through both sidebands and must therefore be accounted for twice.

Equation 5.3 can be solved with respect to the unknown receiver noise temperature:

$$T_{rec.,dsb} = \frac{T_{hot} - Y \cdot T_{cold}}{Y - 1} \quad (5.4)$$

We now have a way of directly estimating the receiver input noise temperature using Y-factor measurements. In Table 5.1 values of the receiver noise temperature versus Y-factor are shown. By adding an attenuator with a known attenuation at the ambient temperature T_{amb} in between the mixer and the LNA, we can also determine the mixer equivalent noise temperature and conversion gain. The input noise temperature of an attenuator with loss L_{att} equals to [76]:

$$T_{att} = T_{amb}(L_{att} - 1) \quad (5.5)$$

The input noise temperature for a 3 dB attenuator in room temperature is 290 K. Placed in between the mixer and the LNA in a receiver system it also increases the contribution of the LNA input noise temperature to the output of the mixer by a factor of two. The receiver input noise temperature can now be rewritten as:

$$T_{rec,ssb,att} = T_{mix,ssb} + L_{mix}(T_{amb}(L_{att} - 1) + L_{att} \cdot T_{lna}) \quad (5.6)$$

By subtracting the nominally measured receiver noise temperature $T_{rec.,ssb}$ from the one using a 3 dB attenuator $T_{rec.,ssb,att}$ setting $L_{att}=2$ and solving the equation for L_{mix} , we can get an explicit expression for the mixer conversion loss as a function of the difference in measured

Table 5.2: Mixer conversion loss L_{mix} versus measured receiver noise difference Δ with and without a 3 dB attenuator assuming a T_{lna} of 50 K and 100 K respectively.

Δ [K]	$L_{mix,50K}$ [dB]	$L_{mix,100K}$ [dB]
1000	5.7	5
1250	7.1	6.3
1500	8.6	7.5
1750	10	8.8
2000	11.4	10

receiver noise temperature and the LNA equivalent noise temperature.

$$L_{mix} = \frac{T_{rec,ssb,att} - T_{rec,ssb}}{T_{amb} + T_{lna}} \quad (5.7)$$

In Table 5.2 values for the mixer conversion loss versus difference in measured receiver noise temperature are shown.

If we know the IF chain noise temperature, we can easily calculate the equivalent mixer input noise by subtracting the IF noise contribution. A first approximation is to assume matched conditions between the LNA and mixer and that additional IF noise from backend can be neglected. In Fig. 5.2 the extracted mixer noise is plotted over IF frequency. In this particular setup a coaxial packaged Chalmers 1-14 GHz LNA module (design by Niklas Wadefalk), with 50 K to 100 K noise temperature and 34 dB to 37 dB gain was used together with a 1.5 GHz to 9 GHz YIG filter from Micro Lambda Wireless Inc. with about 40 MHz bandwidth. A resonance slightly above 11 GHz coming from the YIG can be observed in the measurement.

Additional broadband IF amplifiers from MITEQ and a power meter were also used. A matlab (or labview) interface was then used for data readout and tuning of the YIG filter and speed of the chopper wheel. No thermal stabilisation of any components was used other than the heater of the YIG filter.

5.2 Image rejection measurements

A good way of measuring the image rejection is to use a CW signal at the RF frequency. A single tone multiplier chain can be used or, as was done in these measurements, a comb generator, with a spurious response generating all the harmonics of the fundamental pumping frequency (typically 11 GHz - 18 GHz). For an IQ-mixer setup the

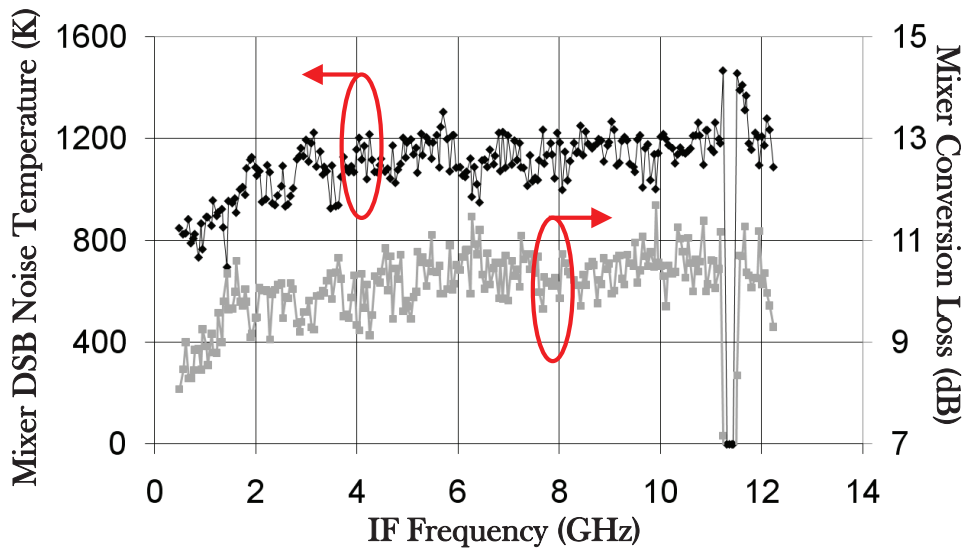


Fig. 5.2: Measured equivalent mixer DSB input noise and conversion loss at 158 GHz and 3.6 dBm of LO frequency and power respectively.

phase and amplitude of the I and Q signals could be compared using an oscilloscope and the corresponding image rejection could be calculated. However the large IF bandwidth of the mixer (4 GHz - 21 GHz) requires the use of an additional IF downconverter chain complicating the setup. Instead an IF 90 degree hybrid was connected to the IQ-mixer forming a sideband separating mixer, and the signal power levels at the two IF outputs were instead compared, giving a direct measure of the image rejection. This of course includes the unbalance in the IF hybrid, which in our case can be considered as negligible as the mixer unbalance is relatively large.

The measured 2SB receiver consisted of two separate mixers with integrated LNA's and separate RF and LO hybrid modules. Two mechanical phase tuners were connected to each mixer IF port and phase matched semirigid coaxial cables were connected to various IF hybrids together covering the 2-18 GHz band. The image rejection was optimized in 3 GHz bands, by using only phase tuning, no amplitude tuning was used. The measured image rejection is presented in Fig. 5.3. A simple amplitude tuning could be applied by using fixed IF attenuators of equal length or by switching LO feeding port at the LO hybrid, however the main unbalance seem to be in phase, with up to 60 degrees compensation needed.

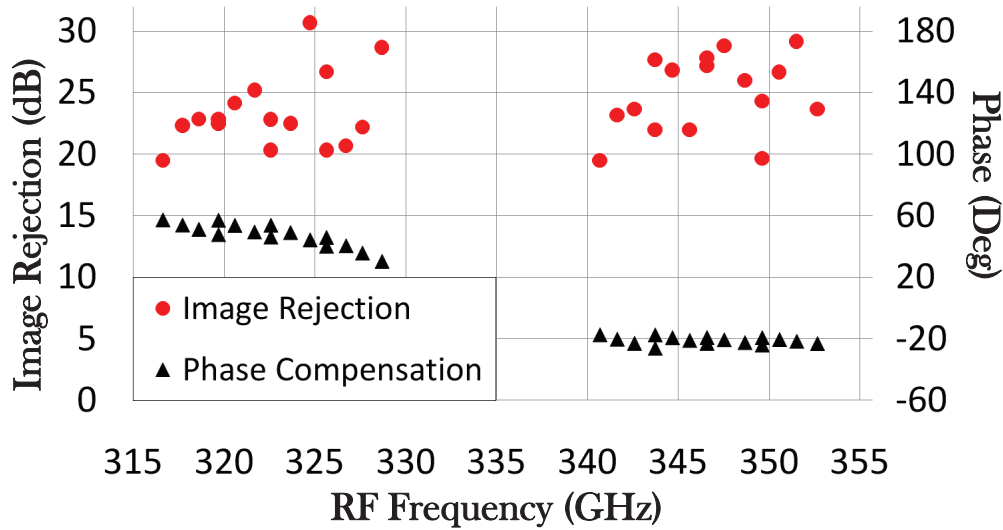


Fig. 5.3: Measured image rejection at 168 GHz LO frequency, using first order phase compensation in 3 GHz IF bands.

5.3 CW conversion loss measurements

For verification of the conversion loss measurements using the Y-factor measurement method, a CW measurement was done. The RF CW source consisted of different prototype W-band multiplier chain setups that were developed for the ALMA Water Vapor Radiometer (WVR). The most powerful multiplier module was comprised of two WR-08 waveguide packaged series connected amplifier modules (Hittite AUH-317 amplifier chip from Velocium, Northrop Grumman) and a passive x3 multiplier module with WR-08 waveguide output interface and a coaxial input interface at around 30 GHz, capable of producing more than 80 mW of output power over the 80 GHz to 90 GHz frequency range, paper [E,F].

A VDI high power Schottky doubler module (WR-10 to WR-05) followed by a medium power VDI Schottky doubler (WR-05 to WR-2.8) was then used for multiplication up to 300 GHz. The output power of the specific W-band module used in the setup was not high enough to saturate the VDI x4 chain leading to large ripple in the final output power.

By the use of a spectrum analyser the purity of the IF signal could be verified. A power meter was then used for automated measurements enabling frequency sweeps. In Fig. 5.4 the measured mixer conversion loss is shown. We see that the measured conversion loss is within about 2

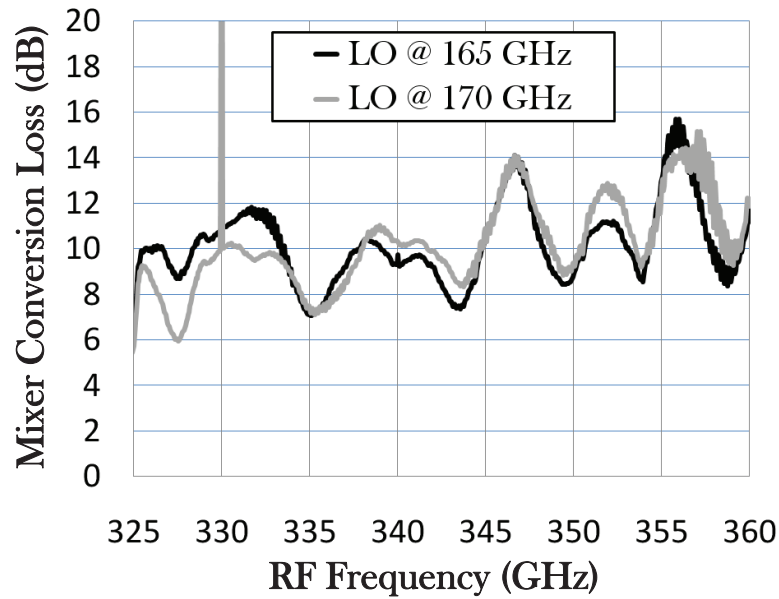


Fig. 5.4: Measured conversion loss at 160 GHz and 170 GHz LO frequency using a RF CW source.

dB of the conversion loss level in the Y-factor measurements. There is a clear periodic ripple in the response in both curves, which were measured at different LO frequencies. This points to a large RF standing wave effecting the accuracy of this measurement. By changing the setup to include an isolator or attenuator the RF standing wave could potentially be decreased improving the accuracy of this measurement.

Chapter 6

Conclusions and future outlook

In this thesis work the goal has been to develop practical submm-wave Schottky diode mixers with improved functionality, comparing with existing commercially available mixers. This has involved various aspects of mechanical manufacturing and design, electrical modeling, circuit design and manufacturing, assembly and device and circuit characterisation. A simple and clear design methodology has also been developed for subharmonic mixers employing antiparallel diodes. The availability of commercial Schottky devices, an in-house circuit process as well as in-house manufacturing of high precision mechanics has played a key role for this development.

The main scientific contribution of this work, has been the development of novel and practical sideband separation concepts employing subharmonic Schottky diode mixers Papers [A, D, E]. The demonstration of two novel and compact concepts for sideband separation using waveguide packaged subharmonic mixers has been important, as efficient 2SB operation can now for the first time be considered for atmospheric sensing instruments as well as for submillimetre wave instrumentation in general.

As a side result two novel differential phase shifter topologies have been proposed and demonstrated Paper [B]. The phase shifters have interesting features such as small lateral extension and possibility to utilise the longitudinal distribution of the component for more efficient layouts suitable for MMIC and TMIC applications. Finally a novel approach of applying TRL-calibration at submillimetre wave frequencies has been proposed and demonstrated which makes more accurate characterisation of THz-devices and circuits possible, Paper [C]. This should allow for better prediction of device parameters and lead to improved

performance of THz circuits and systems.

In general the prospects of developing Schottky diode technology based receiver systems for atmospheric observations and planetary missions seem very promising looking at the technology development roadmaps for the coming 10+ years. As the feasibility of using transistor technology is expected to be pushed up to at least 300 GHz the focus for Schottky development will be at submillimetre wave wavelengths from 300 GHz and up, improving efficiency and functionality of receiver systems. We will see a continuous trend of integrating multiple receiver functions in to single waveguide modules and on chip integration using TMIC technology for the realisation of compact, low weight, state of the art heterodyne receivers and systems. This will enable new instrument configurations and measurement methods and eventually lead to better climate and weather forecasts as well as understanding of the atmospheric processes. Another consequence will be that other emerging applications in the fields of security, medicine and communication will have greater probability to evolve and reach the market. If so, we will see a revolution of new applications closing the THz gap and opening the THz window for good.

Acknowledgements

First of all I would like to thank my two mentors, coaches and supervisors Jan Stake and Anders Emrich, for your perseverance and support. As always a project such as this is the result of an inspirational environment created by the very people working in it. This is where seeds for new ideas and innovations are borne and this is where you find the expertise and help when needed. With those words said, I would like to thank all my colleagues and friends at the Department of Microtechnology and Nanoscience, at Omnisys Instruments AB and at the Department of Radio and Space Science. You have contributed in sweat, occasionally with tears but hopefully not in blood to this work.

Thanks to my family for always being there even when I have been completely elsewhere.

I would finally like to acknowledge the financing institutions and collaboration partners. This work has been supported in part by the Swedish Research Council (VR) under grant no. 2005-2855 and has at a later stage also been carried out in the GigaHertz Centre in a joint project in part financed by the Swedish Governmental Agency of Innovation Systems (VINNOVA), Chalmers University of Technology, Wasa Millimeter Wave AB, Omnisys Instruments AB and SP Technical Research Institute of Sweden.

Bibliography

- [1] I. Mehdi, S. Marazita, D. Humphrey, T.-H. Lee, R. Dengler, J. Oswald, A. Pease, S. Martin, W. Bishop, T. Crowe, and P. Siegel, “Improved 240-GHz subharmonically pumped planar Schottky diode mixers for space-borne applications,” *IEEE Transactions on Microwave Theory and Techniques*, vol. 46, no. 12, pp. 2036–2042, Dec. 1998.
- [2] T. Crowe, W. Bishop, D. Porterfield, J. Hesler, and I. Weikle, R.M., “Opening the terahertz window with integrated diode circuits,” *IEEE Journal of Solid-State Circuits*, vol. 40, no. 10, pp. 2104–2110, Oct. 2005.
- [3] S. Marazita, W. Bishop, J. Hesler, K. Hui, W. Bowen, and T. Crowe, “Integrated GaAs Schottky mixers by spin-on-dielectric wafer bonding ,” *IEEE Transactions on Electron Devices*, vol. 47, no. 6, pp. 1152–1157, June 2000.
- [4] T. Crowe, R. Mattauch, H. Roser, W. Bishop, W. Peatman, and X. Liu, “GaAs Schottky diodes for THz mixing applications,” *Proceedings of the IEEE*, vol. 80, no. 11, pp. 1827–1841, Nov. 1992.
- [5] European Space Agency, ESA SP-1313/5 Candidate Earth Explorer Core Missions Reports for Assessment: PREMIER Process Exploration through Measurements of Infrared and millimetre-wave Emitted Radiation, 2008, ISBN 978-92-9221-406-7, ISSN 0379-6566 .
- [6] P. Siegel, “THz Instruments for Space,” *IEEE Transactions on Antennas and Propagation*, vol. 55, no. 11, pp. 2957–2965, Nov. 2007.
- [7] T. Phillips and J. Keene, “Submillimeter astronomy [heterodyne spectroscopy],” *Proceedings of the IEEE*, vol. 80, no. 11, pp. 1662–1678, Nov. 1992.
- [8] A. Wootten and A. Thompson, “The Atacama Large Millimeter/Submillimeter Array,” *Proceedings of the IEEE*, vol. 97, no. 8, pp. 1463–1471, Aug. 2009.

- [9] J. Kumagal, "Space mountain [submillimeter radio telescopes]," *IEEE Spectrum*, vol. 42, no. 12, pp. 12–14, Dec. 2005.
- [10] D. Doyle, G. Pilbratt, and J. Tauber, "The Herschel and Planck Space Telescopes," *Proceedings of the IEEE*, vol. 97, no. 8, pp. 1403–1411, Aug. 2009.
- [11] P. Richards, "Cosmic Microwave Background experiments - past, present and future," in *Joint 32nd International Conference on Infrared and Millimeter Waves and the 15th International Conference on Terahertz Electronics, IRMMW-THz.*, Sept. 2007, pp. 12–15.
- [12] Jet Propulsion Laboratory, California Institute of Technology, <http://spec.jpl.nasa.gov/> .
- [13] P. Siegel, "Terahertz technology," *IEEE Transactions on Microwave Theory and Techniques*, vol. 50, no. 3, pp. 910–928, Mar. 2002.
- [14] D. Glaab, S. Boppel, A. Lisauskas, U. Pfeiffer, E. Ojefors, and H. G. Roskos, "Terahertz heterodyne detection with silicon field-effect transistors," *Applied Physics Letters*, vol. 96, no. 4, pp. 042106–042106–3, Jan. 2010.
- [15] M. Kroug, A. Endo, T. Tamura, T. Noguchi, T. Kojima, Y. Uzawa, M. Takeda, Z. Wang, and W. Shan, "SIS Mixer Fabrication for ALMA Band10," *IEEE Transactions on Applied Superconductivity*, vol. 19, no. 3, pp. 171–173, June 2009.
- [16] S. Cherednichenko, V. Drakinskiy, T. Berg, P. Khosropanah, and E. Kollberg, "Hot-electron bolometer terahertz mixers for the Herschel Space Observatory," *Review of Scientific Instruments*, vol. 79, no. 3, pp. 034501–034501–10, Mar. 2008.
- [17] W. Deal, X. Mei, V. Radisic, B. Bayuk, A. Fung, W. Yoshida, P. Liu, J. Uyeda, L. Samoska, T. Gaier, and R. Lai, "A New Sub-Millimeter Wave Power Amplifier Topology Using Large Transistors," *IEEE Microwave and Wireless Components Letters*, vol. 18, no. 8, pp. 542–544, Aug. 2008.
- [18] J. Ward, G. Chattopadhyay, J. Gill, H. Javadi, C. Lee, R. Lin, A. Maestrini, F. Maiwald, I. Mehdi, E. Schlecht, and P. Siegel, "Tunable broadband frequency-multiplied terahertz sources," in *33rd International Conference on Infrared, Millimeter and Terahertz Waves, IRMMW-THz*, Sept. 2008, pp. 1–3.
- [19] H.-W. Hubers, "Terahertz Heterodyne Receivers," *IEEE Journal of Selected Topics in Quantum Electronics*, vol. 14, no. 2, pp. 378–391, Mar.-Apr. 2008.

- [20] O. Koistinen, H. Valmu, A. Raisanen, J. Talvela, and M. Halikainen, "A Radiometer for Ground-Based Detection of Stratospheric Ozone at 110 GHz," in *22nd European Microwave Conference*, vol. 2, Sept. 1992, pp. 1231–1233.
- [21] B. Thomas, P. G. Huggard, B. Alderman, B. P. Moyna, M. L. Oldfield, B. N. Ellison, and D. N. Matheson, "Integrated Heterodyne Receivers for MM SubMM Atmospheric Remote Sensing," in *The Institution of Engineering and Technology Seminar on MM-Wave Products and Technologies*, Nov. 2006, pp. 13–18.
- [22] C. Groppi, R. Kursinski, D. Ward, A. Otarola, K. Sammler, M. Schein, S. Al Banna, B. Wheelwright, S. Bell, W. Bertiger, M. Miller, and H. Pickett, "ATOMMS: the Active Temperature, Ozone and Moisture Microwave Spectrometer," in *Twentieth International Symposium on Space Terahertz Technology, Charlottesville*, Apr. 2009, pp. 167–173.
- [23] I. Yoshihisa, T. Manabe, S. Ochiai, H. Masuko, T. Yamagami, Y. Saito, N. Izutsu, T. Kawasaki, M. Namiki, K. Sato, and I. Murata, "A balloon-borne 620-650 GHz SIS receiver for atmospheric observations," in *IEEE International Geoscience and Remote Sensing Symposium, IGARSS*, vol. 1, July 2005, p. 4.
- [24] Japan Aerospace Exploration Agency, JAXA, <http://www.isas.jaxa.jp/e/enterp/rockets/sounding/index.shtml>.
- [25] "Global observations of middle atmospheric water vapour by the Odin satellite: An overview", journal =.
- [26] N. Skou and D. L. Vine, *Microwave Radiometer Systems: Design and Analysis, Second Edition*. Artech House, 2006.
- [27] M. Griffin, G. Pilbratt, T. de Graauw, and A. Poglitsch, "The Herschel Space Observatory," in *33rd International Conference on Infrared, Millimeter and Terahertz Waves, IRMMW-THz*, Sept. 2008, pp. 1–2.
- [28] H. Sugita, T. Nakagawa, H. Murakami, A. Okamoto, H. Nagai, M. Murakami, K. Narasaki, and M. Hirabayashi, "Cryogenic infrared mission "JAXA/SPICA" with advanced cryocoolers," *Cryogenics*", vol. 46, no. 2-3, pp. 149–157, 2006, 2005 Space Cryogenics Workshop. [Online]. Available: <http://www.sciencedirect.com/science/article/B6TWR-4J2TVTB-1/2/d2bcdb76880a7f68694e738f23d70a65>
- [29] M. Cohn, J. Degenford, and B. Newman, "Harmonic Mixing with an Anti-Parallel Diode Pair," in *MTT International Microwave Symposium Digest*, vol. 74, no. 1, June 1974, pp. 171–172.

- [30] I.-H. Lin, K. Leong, C. Caloz, and T. Itoh, "Dual-band sub-harmonic quadrature mixer using composite right/left-handed transmission lines," *IEE Proceedings - Microwaves, Antennas and Propagation*, vol. 153, no. 4, pp. 365–375, Aug. 2006.
- [31] T. Yamaji, H. Tanimoto, and H. Kokatsu, "An I/Q active balanced harmonic mixer with IM2 cancelers and a 45 deg; phase shifter," in *IEEE International Solid-State Circuits Conference, Digest of Technical Papers*, Feb. 1998, pp. 368–369, 466.
- [32] V. Vassilev, D. Henke, I. Lapkin, O. Nyström, R. Monje, A. Pavolotsky, and V. Belitsky, "Design and Characterization of a 211 GHz Sideband Separating Mixer for the APEX Telescope," *IEEE Microwave and Wireless Components Letters*, vol. 18, no. 1, pp. 58–60, Jan. 2008.
- [33] B. Thomas, S. Rea, B. Moyna, B. Alderman, and D. Matheson, "A 320-360 GHz Subharmonically Pumped Image Rejection Mixer Using Planar Schottky Diodes," *IEEE Microwave and Wireless Components Letters*, vol. 19, no. 2, pp. 101–103, Feb. 2009.
- [34] V. Vassilev, V. Belitsky, D. Urbain, and S. Kovtonyuk, "A new 3-dB power divider for millimeter-wavelengths," *IEEE Microwave and Wireless Components Letters*, vol. 11, no. 1, pp. 30–32, Jan. 2001.
- [35] P. Lehtikainen, J. Mallat, P. Piironen, A. Lehto, J. Tuovinene, and A. V. Räisänen, "A 119 GHz planar Schottky diode mixer for a space application," *International Journal of Infrared and Millimeter Waves*, vol. 17, pp. 807–818, May 1996.
- [36] P. Siegel, R. Dengler, I. Mehdi, W. Bishop, and T. Crowe, "A 200 GHz planar diode subharmonically pumped waveguide mixer with state-of-the-art performance," in *IEEE MTT-S International Microwave Symposium Digest*, June 1992, pp. 595–598, Vol.2.
- [37] W. Y. Ali-Ahmad, W. L. Bishop, T. W. Crowe, and G. M. Rebeiz, "A 250 GHz planar low noise Schottky receiver," *International Journal of Infrared and Millimeter Waves*, vol. 14, pp. 737–748, Apr. 1993.
- [38] S. Rea, B. Thomas, and D. Matheson, "A 320-360 GHz Sub-Harmonically pumped Image-Rejection Mixer for earth observation applications," Sept. 2008, p. 1.
- [39] J. Hesler, K. Hui, S. He, and T. Crowe, "A Fixed-Tuned 400 GHz Subharmonic Mixer using Planar Schottky Diodes," in *Tenth International Symposium on Space Terahertz Technology, Charlottesville*, Mar. 1999, pp. 95–99.

- [40] B. Thomas, A. Maestrini, and G. Beaudin, "A low-noise fixed-tuned 300-360-GHz sub-harmonic mixer using planar Schottky diodes," *IEEE Microwave and Wireless Components Letters*, vol. 15, no. 12, pp. 865–867, Dec. 2005.
- [41] K. Hui, J. Hesler, D. Kurtz, W. Bishop, and T. Crowe, "A micro-machined 585 GHz Schottky mixer," *IEEE Microwave and Guided Wave Letters*, vol. 10, no. 9, pp. 374–376, Sept. 2000.
- [42] M. Boheim, L.-P. Schmidt, J. Ritter, V. Brankovic, R. Beyer, F. Arndt, U. Klein, K. Kunzi, G. Schwaab, and T. W. Crowe, "A New 140 GHz Planar Diode Finline Mixer for Radiometer Applications," in *24th European Microwave Conference*, vol. 1, Sept. 1994, pp. 664–669.
- [43] W. Bishop, K. McKinney, R. Mattauch, T. Crowe, and G. Green, "A Novel Whiskerless Schottky Diode for Millimeter and Submillimeter Wave Application," in *MTT-S International Microwave Symposium Digest*, vol. 87, no. 2, June 1987, pp. 607–610.
- [44] S. Gearhart, J. Hesler, W. Bishop, T. Crowe, and G. Rebeiz, "A wide-band 760-GHz planar integrated Schottky receiver," *IEEE Microwave and Guided Wave Letters*, vol. 3, no. 7, pp. 205–207, July 1993.
- [45] J. Hesler, "Broadband Fixed-Tuned Subharmonic Receivers to 640 GHz," in *Eleventh International Symposium on Space Terahertz Technology*, 2000, pp. 3–5.
- [46] B. Moyna, C. Mann, B. Ellison, M. Oldfield, D. Matheson, and T. Crowe, "Broadband space-qualified subharmonic mixers at 183 GHz with low local oscillator power requirements," in *2nd ESA Workshop on MM-Wave Technology Applications: Antennas, Circuits Systems, Espoo, Finland*, May 1998, pp. 3–5.
- [47] S. Vogel, "Design and measurements of a novel subharmonically pumped millimeter-wave mixer using two single planar Schottky-barrier diodes," *IEEE Transactions on Microwave Theory and Techniques*, vol. 44, no. 6, pp. 825–831, June 1996.
- [48] J. Hesler, D. Porterfield, W. Bishop, T. Crowe, and P. Racette, "Development of compact broadband receivers at submillimeter wavelengths," in *IEEE Aerospace Conference Proceedings*, vol. 2, Mar. 2004, pp. 735–740, Vol.2.
- [49] J. Hesler, W. Hall, T. Crowe, I. Weikle, R.M., J. Deaver, B.S., R. Bradley, and S.-K. Pan, "Fixed-tuned submillimeter wavelength waveguide mixers using planar Schottky-barrier diodes," *IEEE Transactions on Microwave Theory and Techniques*, vol. 45, no. 5, pp. 653–658, May 1997.

- [50] I. Mehdi, S. Marazita, D. Humphrey, T.-H. Lee, R. Dengler, J. Oswald, A. Pease, S. Martin, W. Bishop, T. Crowe, and P. Siegel, “Improved 240-GHz subharmonically pumped planar Schottky diode mixers for space-borne applications,” *IEEE Transactions on Microwave Theory and Techniques*, vol. 46, no. 12, pp. 2036–2042, Dec. 1998.
- [51] D. Porterfield, J. Hesler, T. Crowe, W. Bishop, and D. Woolard, “Integrated terahertz transmit/receive modules,” in *33rd European Microwave Conference*, vol. 3, Oct. 2003, pp. 1319–1322, Vol.3.
- [52] S. Marazita, K. Hui, J. Hesler, W. Bishop, and T. Crowe, “Progress in Submillimeter Wavelength Integrated Mixer Technology,” in *Tenth International Symposium on Space Terahertz Technology*, Charlottesville, Mar. 1999, pp. 95–99.
- [53] Virginia Diodes Inc., www.virginiadiodes.com.
- [54] N. Erickson, “A Very Low-Noise Single-Sideband Receiver for 200–260 GHz,” *IEEE Transactions on Microwave Theory and Techniques*, vol. 33, no. 11, pp. 1179–1188, Nov. 1985.
- [55] B. Thomas, P. G. Huggard, B. Alderman, B. P. Moyna, M. L. Oldfield, B. N. Ellison, and D. N. Matheson, “Integrated Heterodyne Receivers for MM SubMM Atmospheric Remote Sensing,” in *The Institution of Engineering and Technology Seminar on MM-Wave Products and Technologies*, Nov. 2006, pp. 13–18.
- [56] S. B. Rozanov, A. N. Lukin, and S. V. Solomonov, “Low-noise cooled planar Schottky diode receivers for ground-based spectral ozone measurements at 142 GHz,” *International journal of infrared and millimeter waves*, vol. 19, no. 2, pp. 195–222, 1998.
- [57] S. Cherednichenko, V. Drakinskiy, T. Berg, P. Khosropanah, and E. Kollberg, “Hot-electron bolometer terahertz mixers for the Herschel Space Observatory,” *Review of Scientific Instruments*, vol. 79, no. 3, pp. 034 501–034 501–10, Mar. 2008.
- [58] W. Zhang, P. Khosropanah, J. R. Gao, E. L. Kollberg, K. S. Yngvesson, T. Bansal, R. Barends, and T. M. Klapwijk, “Quantum noise in a terahertz hot electron bolometer mixer,” *Applied Physics Letters*, vol. 96, no. 11, pp. 111 113–111 113–3, Mar. 2010.
- [59] A. Tessmann, A. Leuther, M. Kuri, H. Massler, M. Riessle, H. Essen, S. Stanko, R. Sommer, M. Zink, R. Stibal, W. Reinert, and M. Schlechtweg, “220 GHz Low-Noise Amplifier Modules for Radiometric Imaging Applications,” in *The 1st European Microwave Integrated Circuits Conference*, Sept. 2006, pp. 137–140.

- [60] H. Wang, R. Lai, Y.-L. Kok, T.-W. Huang, M. Aust, Y. Chen, P. Siegel, T. Gaier, R. Dengler, and B. Allen, "A 155-GHz monolithic low-noise amplifier," *IEEE Transactions on Microwave Theory and Techniques*, vol. 46, no. 11, pp. 1660–1666, Nov. 1998.
- [61] R. Lai, W. Deal, V. Radisic, K. Leong, X. Mei, S. Sarkozy, T. Gaier, L. Samoska, and A. Fung, "Sub-MMW active integrated circuits based on 35 nm InP HEMT technology," in *IEEE International Conference on Indium Phosphide Related Materials, IPRM*, May 2009, pp. 185–187.
- [62] P. Kangaslahti, D. Pukala, T. Gaier, W. Deal, X. Mei, and R. Lai, "Low noise amplifier for 180 GHz frequency band," in *IEEE MTT-S International Microwave Symposium Digest*, June 2008, pp. 451–454.
- [63] S. Gunnarsson, N. Wadefalk, J. Svedin, S. Cherednichenko, I. Angelov, H. Zirath, I. Kallfass, and A. Leuther, "A 220 GHz Single-Chip Receiver MMIC With Integrated Antenna," *IEEE Microwave and Wireless Components Letters*, vol. 18, no. 4, pp. 284–286, Apr. 2008.
- [64] H. Zirath, N. Wadefalk, R. Kuzhuharov, S. Gunnarson, S. Cherednichenko, I. Angelov, M. Abbasi, B. Hansson, V. Vassilev, J. Svedin, S. Rudner, I. Kallfass, and A. Leuther, "Integrated receivers up to 220 GHz utilizing GaAs-mHEMT technology," in *IEEE German Microwave Conference, GeMMIC*, Mar. 2010, pp. 1–2.
- [65] E. Kollberg and A. Rydberg, "Quantum-barrier-varactor diodes for high-efficiency millimetre-wave multipliers," *Electronics Letters*, vol. 25, no. 25, pp. 1696–1698, Dec. 1989.
- [66] K. Yhland, "Simplified Analysis of Resistive Mixers," *IEEE Microwave and Wireless Components Letters*, vol. 17, no. 8, pp. 604–606, Aug. 2007.
- [67] W. Kelly and G. Wrixon, "Conversion Losses in Schottky-Barrier Diode Mixers in the Submillimeter Region," *IEEE Transactions on Microwave Theory and Techniques*, vol. 27, no. 7, pp. 665–672, July 1979.
- [68] M. McColl, "Conversion Loss Limitations on Schottky-Barrier Mixers (Short Papers)," *IEEE Transactions on Microwave Theory and Techniques*, vol. 25, no. 1, pp. 54–59, Jan. 1977.
- [69] W. Schottky, *Phys. Z.*, vol. 41, p. 570, 1940.
- [70] F. Braun, "Über die stromleitung durch schwefelmetalle," *Annalen der Physik*, vol. 229, no. 12, pp. 556–563, 1875.

- [71] A. Cowley and S. Sze, “Surface States and Barrier Height of Metal-Semiconductor Systems,” *Journal of Applied Physics*, vol. 36, no. 10, pp. 3212–8, 1965.
- [72] S. Sze, C. Crowell, and D. Kahng, “Photoelectric Determination of Image Force Dielectric Constant For Hot Electrons in Schottky Barriers,” *Journal of Applied Physics*, vol. 35, no. 8, pp. 2534–8, 1964.
- [73] J. Bardeen, “Surface States and Rectification at a Metal Semiconductor Contact,” *Physical Review*, vol. 71, no. 10, pp. 717–727, 1947.
- [74] J. L. Hesler, “Planar Schottky Diodes in Submillimeter-Wavelength Waveguide Receivers,” Ph.D. dissertation, School of Engineering and Applied Science, University of Virginia, Charlottesville, United States, 1996.
- [75] H. Xu, G. Schoenthal, L. Liu, Q. Xiao, J. Hesler, and R. Weikle, “On Estimating and Canceling Parasitic Capacitance in Submillimeter-Wave Planar Schottky Diodes,” *IEEE Microwave and Wireless Components Letters*, vol. 19, no. 12, pp. 807–809, Dec. 2009.
- [76] S. A. Maas, *Noise in linear and nonlinear circuits*.
- [77] T. W. Crowe, “Modeling and optimization of GaAs Schottky barrier mixer diodes,” Ph.D. dissertation, School of Engineering and Applied Science, University of Virginia, Charlottesville, United States, 1986.
- [78] Virginia Diodes Inc., <http://www.virginiadiodes.com> .
- [79] E. Schlecht, J. Gill, R. Dengler, R. Lin, R. Tsang, and I. Mehdi, “A Unique 520-590 GHz Biased Subharmonically-Pumped Schottky Mixer,” *IEEE Microwave and Wireless Components Letters*, vol. 17, no. 12, pp. 879–881, Dec. 2007.
- [80] T.-H. Lin and R.-B. Wu, “A Broadband Microstrip-to-Waveguide Transition with Tapered CPS Probe,” in *32nd European Microwave Conference*, Sept. 2002, pp. 1–4.
- [81] Z. Tong, A. Stelzer, W. Menzel, C. Wagner, R. Feger, and E. Kolmhofer, “A wide band transition from waveguide to differential microstrip lines,” in *Asia-Pacific Microwave Conference, APMC*, Dec. 2008, pp. 1–4.
- [82] W. R. Deal, X. B. Mei, V. Radisic, K. Leong, S. Sarkozy, B. Gorospe, J. Lee, P. H. Liu, W. Yoshida, J. Zhou, M. Lange,

- J. Uyeda, and R. Lai, "Demonstration of a 0.48 THz Amplifier Module Using InP HEMT Transistors," *IEEE Microwave and Wireless Components Letters*, vol. PP, no. 99, pp. 1–3, 2010.
- [83] G. Ponchak and R. Simons, "A new rectangular waveguide to coplanar waveguide transition," in *IEEE MTT-S International Microwave Symposium Digest*, May 1990, pp. 491–492, Vol.1.
- [84] N. Erickson, "A Very Low-Noise Single-Sideband Receiver for 200-260 GHz," *IEEE Transactions on Microwave Theory and Techniques*, vol. 33, no. 11, pp. 1179–1188, Nov. 1985.
- [85] A. R. Kerr, M. J. Feldman, and S.-K. Pan, "Receiver Noise Temperature, the Quantum Noise Limit, and the Role of the Zero-Point Fluctuations," in *8th Int. Symp. on Space Terahertz Tech.*, Mar. 1997, pp. 101–111.

Paper A

A 170 GHz 45° Hybrid for Submillimeter Wave Sideband Separating Subharmonic Mixers

P. Sobis, J. Stake, and A. Emrich

in *IEEE Microwave and Wireless Components Letters*, vol. 18, no. 10, pp. 680–682, Oct. 2008.

Paper B

High/Low Impedance Transmission Line and Coupled Line Filter Networks for Differential Phase Shifters

P. Sobis, J. Stake, and A. Emrich

submitted to *IEEE Trans. Microw. Theory Tech.*, Feb. 2010.

Paper C

TRL-Calibration and S-Parameter Characterization of Membrane Circuits for Submillimeter Wave Frequencies

H. Zhao, A-Y. Tang, P. Sobis, T. Bryllert, J. Stake, K. Yhland
and J. Stenarson

submitted to *IEEE Microwave and Wireless Components Letters*,
Mar. 2010.

Paper D

Compact 340 GHz Receiver Front-Ends

P. Sobis, T. Bryllert, A. Olsen, J. Vukusic, V. Drakinskiy, S. Cherednichenko, A. Emrich, and J. Stake

in 20th International Symposium on Space Terahertz Technology, ISSTT 2009, Charlottesville, VA, USA, pp. 183–189, Apr. 2009.

Paper E

STEAMR Receiver Chain

P. Sobis, A. Emrich, and M. Hjorth

in 20th International Symposium on Space Terahertz Technology, ISSTT 2009, Charlottesville, VA, USA, pp. 320–325, Apr. 2009.

Paper F

Water Vapor Radiometer for ALMA

A. Emrich, S. Andersson, M. Wannerbratt, P. Sobis, S. Cherednichenko, D. Runesson, T. Ekebrand, M. Krus, C. Tegnander and U. Krus

in 20th International Symposium on Space Terahertz Technology, ISSTT 2009, Charlottesville, VA, USA, pp. 174–177, Apr. 2009.

CHALMERS UNIVERSITY OF TECHNOLOGY
SE-412 96 Göteborg, Sweden
Telephone: +46-(0)31 772 10 00
www.chalmers.se